OPTIMIZATION OF A GENOME-WIDE SCREEN FOR AML RELAPSE GENES

OPTIMIZATION OF A GENOME-WIDE SCREEN FOR CAUSAL POST-CHEMOTHERAPY RELAPSE GENES IN ACUTE MYELOID LEUKEMIA

By
YEONJOON KIM, B.Sc. (Hons)

A Thesis Submitted to the School of Graduate Studies in Partial Fulfillment of the Requirements for the Degree Master of Science

McMaster University MASTER OF SCIENCE (2020) Hamilton, Ontario (Biochemistry and Biomedical Science)

TITLE:	Optimization of a genome-wide screen for causal post-chemotherapy relapse genes in acute myeloid leukemia
AUTHOR:	Yeonjoon Kim, B.Sc. (Hons)
SUPERVISOR:	Dr. Mickie Bhatia
NUMBER OF PAGES:	xi, 64

Lay Abstract

Acute myeloid leukemia (AML) is a fatal blood cancer that blocks the differentiation of stem cells into functional blood cells. Thus, many patients typically die from infections due to the lack of immune cells. Despite the overwhelming rate of relapse and resultant deaths, the treatment method of AML has remained unchanged for decades. With the goal of identifying the causative genes in AML relapse post-chemotherapy, a novel technology called CRISPR-activation was utilized to develop a genome screening method where each human gene is interrogated for potential relapse-conducive characteristics. The developed screening involves upregulating one unique gene per AML cell, transplanting this pool of cells into mice, treating with chemotherapy, and analysing the surviving cells to identify the upregulated genes that allowed cell survival. All parameters to run the screening were tested and optimized, and the workflow of the screening have been reported.

Abstract

Acute myeloid leukemia (AML) is a highly fatal blood cancer that is characterized by disruption of healthy differentiation of stem cells into functional blood cells in the bone marrow. Most patients with AML consequently die from infections due to the lack of immune cells. For decades, the standard method of remission induction for AML has been chemotherapy using an antineoplastic drug known as AraC. However, even after successful remission induction, aggressive, refractory relapse occurs in the majority of patients within 3 years with dismal survival rates. Here, we sought to develop a genome-wide screening approach to determine the causative genes in AML relapse. In the developed procedure, protein-coding genes of the human genome are screened using a leading-edge technology known as CRISPR (clustered regularly interspaced short palindromic repeats) activation screening. This involves usage of a pooled guide RNA library that upregulates a unique gene for each individual AML cell. By treating these cells with AraC in a mouse xenograft model, the bone marrow will gradually be enriched with cells that carry a guide RNA for a relapse-conducive gene. By harvesting and sequencing all enriched guide RNAs at relapse, the causative genes in AML relapse can be determined. All parameters of the *in vivo* CRISPR-activation screen have been optimized, and the workflow from preparation to the end of screening has been detailed. Follow-up studies that will validate the results of the screen have also been described. The long-term goal of this developed screen is to elucidate the mechanisms of AML relapse and find ways to clinically target these pathways in conjunction with standard the AraC-based chemotherapy.

Acknowledgments

First, I would like to express my gratitude for my thesis supervisor, Dr. Mickie Bhatia, for giving me the opportunity and guidance to conduct this research. I was lucky to have a supervisor with such profound enthusiasm for science. Being in your lab was the greatest privilege in my academic career. Thank you for putting up with my mistakes and slow learning curve. To my supervisory committee members, Dr. Ronan Foley, Dr. Brian Leber, and Dr. Andrew McArthur, thank you for your interest in this project and taking time to offer your valuable guidance.

I would also like to acknowledge Dr. Jennifer Reid for her tremendous, selfless contributions to this research and my personal success. I know you are awkward with compliments, but you are an exemplary scientist and I thoroughly enjoyed working with you. I could not have asked for a better teacher.

All members of the Bhatia Program, thank you for all your kindness and moral support. There were some tough times during the graduate student journey, but you made everything better. I wish I could always work with people as friendly and kind as you are. Thank you, Dr. Mio Nakanishi, for teaching me the ropes, your guidance, and always rooting for my success. I wish nothing but the best for you in Japan. My dear friend, Gena Markous, thank you for always keeping me company and brightening my days at the lab. I am glad I had someone who appreciated my quirks and dark humor. I had a blast.

I would like to thank my parents for their unconditional love and support throughout my life. I will forever be indebted to you for all the opportunities you have given me. Lastly, I would like to thank my significant other, Jean Phan, for filling my world with nothing but hope, happiness, and courage.

Table of Contents

List of Figures

List of Tables

List of Abbreviations and Symbols

AGM: Aorta-gonad-mesonephros
AML: Acute myeloid leukemia
AraC: Cytosine arabinoside
araCTP: Arabinosyl cytosine triphosphate
BSD: Blasticidin deaminase gene
Bp: Base pairs
Cas: CRISPR associated proteins
Cas9: CRISPR associated protein 9
CR: Complete remission
CRISPR: Clustered regularly interspaced short palindromic repeats
CRISPRa: CRISPR-activator CRISPR-activation
CRISPR/Cas9: CRISPR and Cas9 protein
crRNA: CRISPR RNA
dCas9: Endonuclease-deactivated Cas9
dCTP: Deoxycytidine triphosphate
DMSO: Dimethyl sulfoxide
DNMT3A: DNA methyl transferase 3A gene
DRD2: Dopamine receptor D2 gene
DSB: Double stranded breakage
E.coli: *Escherichia coli*
EDTA: Ethylenediaminetetraacetic acid
EF-1α: Human elongation factor 1α
FACS: Fluorescence activated cell sorting
FBS: Fetal bovine serum
GOF: Gain of function
GPCR: G-protein-coupled receptor
HEK: Human embryonic kidney
h.i: Heat-inactivated
HSCT: Hematopoietic stem cell transplantation
HSC: Hematopoietic stem cell
HTR4: 5-hydroxytryptamine receptor 4 gene
HygR or *Hph*: hygromycin phosphotrasferase gene
IL2γ_c: Interleukin-2 receptor gamma chain
IMDM: Iscove Modified Dulbecco Media
IV: Intravenous
LB: Lysogeny broth
LOF: Loss of function
LRC: Leukemia regenerating cell
MOI: Multiplicity of infection
MPH: MS2-P65-HSF1
NGS: Next generation sequencing
NOD: Non-obese diabetic
NSG: NOD-SCID-IL2rγ^{null}
nu: Nude mice

PAM: Protospacer adjacent motif
PBS: Phosphate buffered saline
PDX: Patient derived xenograft
PEF: FBS, EDTA, PBS solution
PRKDC: Protein kinase DNA-activated catalytic polypeptide gene
RIGER: RNAi gene enrichment ranking
RNAi: RNA interference
SAMv2: Synergistic activation mediator
SCID: Severe combine immunodeficient
scRNA-seq: Single cell RNA sequencing
sgRNA: Single guide RNA
shRNA: Short hairpin RNA
SRSR: Short regularly spaced repeats
TALEN: Transcription activator-like effector nuclease
TCAG: The Centre for Applied Genomics
tracrRNA: Transactivating RNA
ZFN: Zinc finger nuclease
7AAD: 7-aminoactinomycin D
7+3: 7 days of continuous infusion of AraC with the first 3 concurrent days of anthracycline administration

Declaration of Academic Achievement

The work presented in this thesis was mainly done by the author, Yeonjoon Kim, with contribution from Dr. Jennifer Reid with the subcutaneous/intravenous transplantation of OCI-AML3 cells in mice and subsequent bone marrow aspirates.

1.0 Introduction

The information detailed in this thesis describe the optimized procedures for an *in vivo* genome-wide screen for causative post-chemotherapy relapse genes in acute myeloid leukemia (AML). The biological background of the disease is first described, followed by standard clinical treatment methods for AML, and technology to be utilized for the screen.

1.1 Hematopoiesis

Hematopoiesis is the formation of cellular components of the blood. Hematopoiesis is structured in the form of a hierarchy in which hematopoietic stem cells (HSCs) form the apex. These cells are clonogenic and characterized by their abilities of self-renewal, which is the ability to divide into additional copies to perpetuate themselves, and multilineage differentiation into mature, functional cells (Bryder et al., 2006). Hence, HSCs give rise to all blood cells throughout an organism's life. This ability of HSCs to differentiate into many different specialized cells, termed multipotency, and self renewal become less adept as cells move down the hierarchy. Directly under HSCs in the order of hematopoietic hierarchy are progenitors which are more limited in their self-renewal capability and differentiate into a few types of mature cells. Eventually, cells differentiate into maturity and become specialized in a specific function. Thus, as cells progress further down the hematopoietic hierarchy, their self-renewal capability and cell potency are reduced (Jagannathan-Bogdan & Zon, 2013). Largely, hematopoiesis is divided into two lineages, myeloid and lymphoid, as the HSC differentiates into either a common myeloid progenitor or a common lymphoid progenitor. The myeloid lineage gives rise to erythrocytes (red blood cells), which carry oxygen throughout the body; megakaryocytes, which produce platelets; and granulocytes and monocytes that function as critical immune cells (Jagannathan-Bogdan & Zon, 2013). On the other hand, the lymphoid lineage gives rise to other immune cells such as T cells, B cells, and natural killer cells (Jagannathan-Bogdan & Zon, 2013).

HSCs first arise during embryonic development in a region of the mesoderm called the aorta-gonad-mesonephros (AGM), and gradually migrate to the placenta, spleen, and liver (Wang & Wagers, 2011). Around the time of birth, HSCs colonize in the bone marrow where they are maintained for the rest of the adult life (Wang & Wagers, 2011). Interestingly, HSCs that are intravenously (IV) injected into a lethally irradiated isogenic host rescues the hematopoietic deficiency by clonally reconstituting the hematopoietic hierarchy in the bone marrow (Till & McCulloch, 1961). Similarly, in irradiated immune-compromised mouse models, human HSCs are able to engraft in the bone marrow via intravenous injection (L.D. et al., 2012). The irradiation induces myeloablation, a process by which the bone marrow activity is decreased and the number of cells within is decreased (Duran-Struuck & Dysko, 2009). In both human and mouse model hosts, the intravenously injected HSCs are said to "home" to the bone marrow, a phenomenon that refers to these cells' ability to migrate to the organ of their origin (Caocci et al., 2017).

1.2 Acute myeloid leukemia (AML)

Acute myeloid leukemia (AML) is a highly fatal blood cancer that is characterized by disruption of healthy differentiation of HSCs into functional blood cells, and accumulation of immature, proliferative hematopoietic cells in the bone marrow and peripheral blood (Khwaja et al., 2016; Saultz & Garzon, 2016). It afflicts 3-4 individuals per 100,000 annually in the United

States, resulting in over 10,000 deaths in 2015 alone (De Kouchkovsky & Abdul-Hay, 2016). The hematopoietic differentiation in AML can occur anywhere along the myeloid lineage. For example, a differentiation blockage occurring at the promonocytic stage of the myeloid lineage would lead to a lack of monocytes, ultimately leading to a lack of macrophages. Similarly, a differentiation blockage at the myeloid progenitor stage, which is more upstream in hierarchy, would lead to a lack of red blood cells and platelets. Because of the hematopoietic differentiation blockage, causes of death in AML patients primarily include infections (75%), due to the lack of immune cells, and hemorrhage (24%), due to the lack of platelets (Chang et al., 1976). Today, AML is cured in 35-40% of patients who are 60 years of age or younger, and 5-15% in those who are older (Döhner et al., 2017). The lower cure rate in the older patients is largely attributed to comorbidities and their inability to tolerate intensive chemotherapy (Mohammadi et al., 2015). The poor cure rate in the elderly combined with the fact that they present over 10 times the incidence rate of younger individuals makes AML a particularly devastating disease for the elderly (Almeida & Ramos, 2016).

1.2.1 Treatment of AML

Since the early 1970s, the gold standard in the treatment of AML has been induction chemotherapy based on a drug known as cytarabine, also known as arabinosyl cytosine (AraC) (Döhner et al., 2015). The AraC-based chemotherapy regimen is conventionally called "7+3," which refers to 7 days of continuous infusion of AraC with the first 3 concurrent days of anthracycline administration, typically daunorubicin (Saultz & Garzon, 2016). Arabinosyl cytosine enters the cell by facilitated diffusion and gets phosphorylated into its active form, arabinosyl cytosine triphosphate (araCTP) (Cohen, 1977; Damaraju et al., 2003). The araCTP competes with deoxycytidine triphosphate (dCTP) during DNA replication (Cohen, 1977). If incorporated into the DNA during its synthesis, AraC serves as an inefficient substrate for polymerization and simulates a stalled replication fork (Sampath et al., 2003). If DNA polymerase continues the synthesis, the incorporated AraC molecule acts as a preferred binding site for topoisomerase II, which induces a double strand breakage (Cline & Osheroff, 1999). In both cases, DNA damage sensors ATM, ATR, and DNA-PK recognize these events and activate checkpoint pathways that arrest cell cycle progression, leading to apoptosis (Sampath et al., 2003). Thus, AraC preferentially targets rapidly dividing cells, such as leukemia cells, by arresting the cell cycle in the S phase of mitosis. Complete remission (CR) is generally said to have occurred if the blast (immature cell) count is 5% or less in the bone marrow (De Greef et al., 2005).

The challenge to the treatment of AML is in its relapse rate and the refractory nature of the relapsed disease. Although complete remission is achieved in 58.2% of patients using induction chemotherapy, 79% of these patients experience relapse, and less than 10% of relapse patients survive for 5 years (Bose et al., 2017; Verma et al., 2010). In fit patients up to the age of 65, intensive chemotherapy is used to treat relapsed AML, where higher doses of the same drugs used in induction chemotherapy are used (Robak & Wierzbowska, 2009). Intensive chemotherapy is often followed by consideration of the patient for allogeneic hematopoietic stem cell transplantation (HSCT), where stem cells from a healthy donor are transplanted into the bone marrow of the patient (Bose et al., 2017). However, many factors limit the effectiveness of HSCT as a treatment method for AML, such as availability of donors and comorbidities (Bose et al., 2017).

1.2.2 *In vivo* model of AML

In vivo models of AML consist primarily of mouse models. Leukemia in these mouse models can be induced with various methods, including carcinogen-induced tumours, transgenic animals expressing proto-oncogenes/mutations associated with AML (ex. *PML-RARA, RUNX1-ETO*), and xenograft models that are transplanted with primary patient cells or a leukemia cell line (Almosailleakh & Schwaller, 2019). Of these, the xenograft model is the most widely used. Similar to the ability of donor HSCs to engraft in the bone marrow of a recipient, AML cells can engraft and recapitulate the disease in the bone marrow of mouse models. These mice are commonly irradiated before transplant to partially clear out the bone marrow (Duran-Struuck & Dysko, 2009). In the case of patient derived xenograft mouse models (PDX), immune compromised mice are used to eliminate host versus graft disease (Almosailleakh & Schwaller, 2019). Several immunodeficient mouse strains have been developed for xenograft purposes, including nude (*nu*), severe combine immunodeficient (SCID), non-obese diabetic (NOD), NOD-SCID, and NOD-SCID-IL2rγ^{null} (NSG) strains (L.D. et al., 2012; Theocharides et al., 2016).

The SCID strain carries inactivating mutations in the protein kinase DNA-activated catalytic polypeptide (*PRKDC*) gene, which codes for a protein that is involved in DNA repair pathways (Almosailleakh & Schwaller, 2019). This interrupts a process called immunoglobulin V(D)J gene recombination that must occur in developing lymphocytes to produce mature T and B cells (Roth, 2014). Engraftment rates were further improved by combining the SCID strain with the NOD background to produce NOD SCID mice. This strain is unable to produce B or T cells, and has less natural killer cells and macrophages (Cao et al., 1995). Notably, the NOD SCID strain was found to be able to allow engraftment using fewer primary AML cells, and also preserve the phenotypic and genetic characteristics of the transplanted primary AML cells (Bonnet & Dick, 1997). One step further in the creation of immune compromised strain was the NOD/LtSz-*scid* with *IL2*γ_c^{null} (NSG) strain (Ito et al., 2002). The NSG strain carries deletions in the interleukin-2 receptor gamma chain (*IL2*γ_c), which is critical in the production of functional natural killer cells(Shultz et al., 2005). Thus, the NSG strain is unable to produce T cells, B cells, macrophages, and natural killer cells, and substantially improves engraftment rates by almost eliminating the host immune system (Mambet et al., 2018).

Although the preferred method of transplant for AML cells is the IV injection due to its ability to engraft cells in the bone marrow, the subcutaneous injection method is an alternative transplant method. Subcutaneous injections introduce substances just under the skin and not directly into the bloodstream. When rapidly dividing cells, such as AML cells, are transplanted using a substance called Matrigel as an injection vehicle, the injected cells can form an isolated tumor at the injection site (Almosailleakh & Schwaller, 2019). Because Matrigel remains as a liquid at sub-zero temperatures but turns into a solid at higher temperatures, it can serve as a transplant vehicle when kept cold to allow formation of a solid tumor when cells are incubated inside the mouse at body temperature. The solid tumor then grows by forming vascularization (Almosailleakh & Schwaller, 2019).

In the IV transplant method, chimerism is commonly determined by harvesting cells from the leg bone marrow by mechanical dissociation followed by flow cytometry for the human hematopoietic cell surface marker, hCD45 (except erythrocytes and platelets) (Sanchez et al., 2009). In the subcutaneous transplant method, the solid tumor is isolated and chimerism is measured using the same procedure.

1.3 Tools of genetic perturbation

Studies of the genetic origins of disease and mechanisms of disease progression conventionally employ a method of genetic perturbation, followed by phenotypic analysis. As the most common method of identifying gene function is to disrupt its expression and study the resulting phenotypes (Boettcher & McManus, 2015), loss-of-function genetic perturbation tools have been utilized heavily in research. These tools include zinc finger nuclease (ZFN), transcription activator-like effector nuclease (TALEN), RNA interference (RNAi), and clustered regularly interspaced short palindromic repeats (CRISPR)/Cas9. Of these, the CRISPR/Cas9 technology is most recent and has been rapidly adopted by researchers all over the world due to its precision, cost-efficiency, ease of use, and versatility.

1.3.1 CRISPR/Cas9

In 1987, a group of Japanese scientists discovered a series of interspaced palindromic repeats in the genome of *Escherichia coli* with unknown function (Ishino et al., 1987), which were later also discovered in several other bacteria and archaea (Francisco J. M. Mojica et al., 2000). Discoverers of the latter coined the term, short regularly spaced repeats (SRSR) (Mojica et al., 2000), which was more recently renamed as CRISPR (Jansen et al., 2002). The CRISPR loci always accompanied a certain protein-coding genes which were termed the CRISPR associated proteins (Cas) (Jansen et al., 2002). In 2005, it was discovered that this pair of CRISPR and Cas are a part of the prokaryotic adaptive immune system against viruses, suggested by the fact that the sequences present between the palindromic repeats, termed spacers, matched parts of phage genomes (Mojica et al., 2005). The Cas proteins were also found to carry an endonuclease function, causing double stranded breakages (DSB) at precise locations in DNA (Garneau et al., 2010). Presently, the most characterized and widely used Cas protein is that of the *Streptococcus pyogenes*, called Cas9, due to its simplicity of requiring only one Cas protein (Rodríguez-Rodríguez et al., 2019).

The adaptive immunity conferred by the CRISPR/Cas9 system occurs over multiple steps. In the first step, the host cell attains memory of the invading virus. This occurs by integrating a portion of the viral genome into the CRISPR locus of the bacterial genome as spacer sequences (Garneau et al., 2010). After acquiring spacers, the CRISPR locus is transcribed to produce an RNA strand, called pre-CRISPR RNA (pre-crRNA), with sequences that are homologous to past invading viruses (Garneau et al., 2010). A second RNA strand, called transactivating RNA (tracrRNA), is transcribed from a locus that is upstream of the CRISPR locus (Rodríguez-Rodríguez et al., 2019). The tracrRNA contains a region that is complementary to the repeating sequence of the CRISPR locus, allowing it to bind to the pre-crRNA and form a double stranded RNA molecule (Box et al., 2016). The double stranded RNA gets cleaved by RNaseIII into multiple, individual pieces such that each crRNA-tracrRNA duplex contains only one spacer sequence (Rodríguez-Rodríguez et al., 2019). Each RNA duplex then associates with one Cas9 protein to create an active crRNA-tracrRNA-Cas9 complex (Rodríguez-Rodríguez et al., 2019). Upon invasion by a bacteriophage that has had a part of its genome previously incorporated into the cell as a spacer sequence, the corresponding crRNA-tracrRNA-Cas9 complex binds to the invading viral genome by complementary sequence with the crRNA portion of the complex. The endonuclease activity of Cas9 then induces a double stranded breakage in the viral genome, neutralizing the invasion. However, binding of the complex with the invading viral genome and

the actual endonuclease activity are also conditional upon the viral genome carrying a sequence called the protospacer adjacent motif (PAM) (Mojica et al., 2009). The purpose of the PAM is to distinguish the host's CRISPR locus from the viral genome (Jinek et al., 2012). It is a few nucleotides long (the canonical sequence is 5'-NGG-3', where "N" is any base) and is usually near the site of endonuclease activity (Anders et al., 2014).

1.4 Genome-wide screen

Because of the sheer size of mammalian genomes such as that of humans, interrogating each individual gene at a time to study diseases is impractical. Thus, a method of perturbing sets of genes to study those involved in a particular phenotype have become popular. Of these, studies of genes at a scale that span the entire genome are termed genome-wide screens. Genome-wide screens can also be further classified as either loss-of-function (LOF) or gain-of-function (GOF) based on the mode of perturbation. The GOF screens involve conferring new or enhanced activity of the gene products, applying a selection pressure, followed by sequencing of the enriched genetic perturbations to determine the genes associated with resistance to the selection pressure. A commonly used GOF screening method was cDNA overexpression libraries, but this method led to gene overexpression beyond physiological levels, disruption by endogenous regulation, and high cost of construction, limiting its capability as a genome-wide screening tool (Joung et al., 2017). The LOF screens, on the other hand, involve reducing or eliminating the activity of gene products. The earliest screens were LOF screens that utilized chemical DNA mutagens to perturb genes, but this approach was inefficient and too costly to validate induced mutations (Joung et al., 2017). Succeeding this approach was another LOF screening method known as RNA interference (RNAi), which used RNA molecules to inhibit gene expression or translation. Specifically, the short hairpin RNA (shRNA) was a type of RNAi technology that had revolutionized genome-wide screens with its ease of use (Berns et al., 2004; Boutros et al., 2004; Moffat & Sabatini, 2006; Paddison et al., 2004; Root et al., 2006). In the recent decade, new GOF and LOF genome-wide screening platforms derived from the CRISPR/Cas9 technology have replaced pre-existing screening tools due to their superior efficiency, precision, and cost.

1.5 CRISPR-activation technology (using SAMv2 system)

The CRISPR-activation (CRISPRa) technology is a GOF genetic perturbance method derived from the CRISPR/Cas9 system. It utilizes the ability of the crRNA-tracrRNA-Cas9 complex to home to the target locus by complimentary binding using the spacer sequence (Konermann et al., 2015). In CRISPRa, the Cas9 protein is disabled in its endonuclease activity, which is then termed dCas9, leaving only its function of binding to the target locus as guided by the spacer sequence (Konermann et al., 2015). Activating domains can then be recruited to the target gene locus when made to bind with the dCas9 protein, allowing transcriptional upregulation (Konermann et al., 2015) of the gene.

1.5.1 The SAMv2 system: mechanism and workflow

Developed by a group at the Broad Institute, the two-vector synergistic activation mediator (SAMv2) system is a type of CRISPRa genome-wide screening platform (Figure 1.1A) (Konermann et al., 2015). It involves one vector ("SAMv2 vector") that codes for the spacer

sequence and the dCas9 protein, and another "helper" vector that codes for the activating domains (Konermann et al., 2015). In the SAMv2 system, the crRNA and tracrRNA are fused together for simplicity to form a single guide RNA (sgRNA), which binds with the dCas9 (Konermann et al., 2015). The sgRNA is modified to have a hairpin aptamer that binds to a protein dimer called MS2 (Konermann et al., 2015). The helper vector codes for a complex comprised of MS2, P65, and HSF1 (thus also called the "MPH vector"), where the former allows binding with the sgRNA-dCas9 complex while the latter two are activating domains (Konermann et al., 2015). The dCas9 protein in the SAMv2 system is also inherently bound to an activating domain called VP64 (Konermann et al., 2015). When the "MPH" complex binds to the dCas9 protein via MS2, the P65, HSF1, and VP64 activating domains act synergistically to induce transcriptional upregulation of the target gene (Konermann et al., 2015). The SAMv2 system has a library of 70,290 sgRNAs that target 23,430 human coding genes (4 sgRNA isoforms that target each gene) (Joung et al., 2017).

Both the SAMv2 and MPH vectors carry their own antibiotic resistance selectable marker. The SAMv2 vector carries the blasticidin-S deaminase gene (*BSD*) that confers resistance to the antibiotic, blasticidin (Figure 1.1B, top) (Joung et al., 2017). The product of this gene breaks down the antibiotic using water as a substrate (Yamaguchi et al., 1975). The *BSD* gene is driven by the constitutive promoter, human elongation factor 1α (EF-1α), which also drives the sgRNA and dCas9 sequences (Joung et al., 2017; Qin et al., 2010). The MPH vector carries the hygromycin phosphotransferase gene (*HygR*, or *Hph*) (Figure 1.1B, bottom) (Joung et al., 2017). The product of this gene is a kinase that neutralizes the antibiotic by phosphorylation (Rao et al., 1983). The *HygR* gene is also driven by the constitutive promoter, EF-1α, together with the sequences for MS2, P65, and HSF1 (Joung et al., 2017).

The general workflow of the genome-wide CRISPRa screen using the SAMv2 system is as follows:

1. The MPH vector is transduced into the cells of interest, followed by hygromycin selection
2. The SAMv2 vector is transduced into MPH-expressing cells at a low enough multiplicity of infection (MOI) to ensure 1 or no sgRNA is introduced into each cell, followed by blasticidin selection
3. Cells are transplanted into the model host (for *in vivo* screen)
4. Selection pressure is applied to enrich for cells that have upregulated expression of interested genes
5. Enriched cells are harvested and their genomic DNA (gDNA) is harvested
6. Polymerase chain reaction (PCR) is done on the harvested gDNA to amplify the region of the spacer sequence and prepare the library for next generation sequencing (NGS)
7. Amplified library is sequenced via NGS
8. *In silico* analysis to determine the genes of interest ("candidate genes")

The candidate genes of the screen are those that are enriched in the experimental group relative to the control group.

A

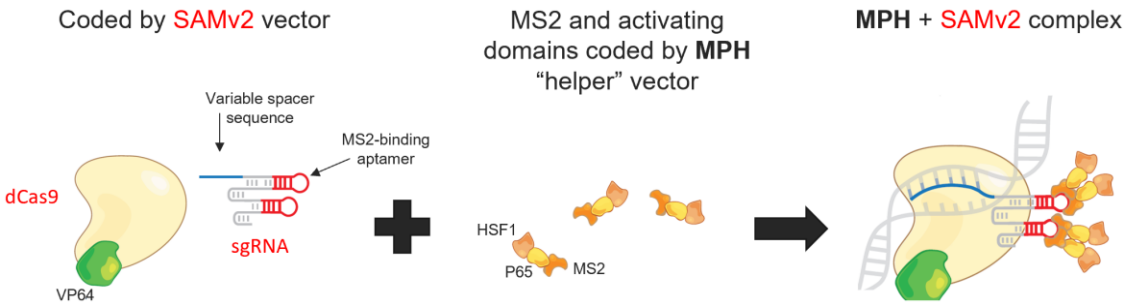
Coded by SAMv2 vector
MS2 and activating domains coded by MPH "helper" vector
MPH + SAMv2 complex
Variable spacer sequence
MS2-binding aptamer
dCas9
sgRNA
VP64
HSF1
P65
MS2

B

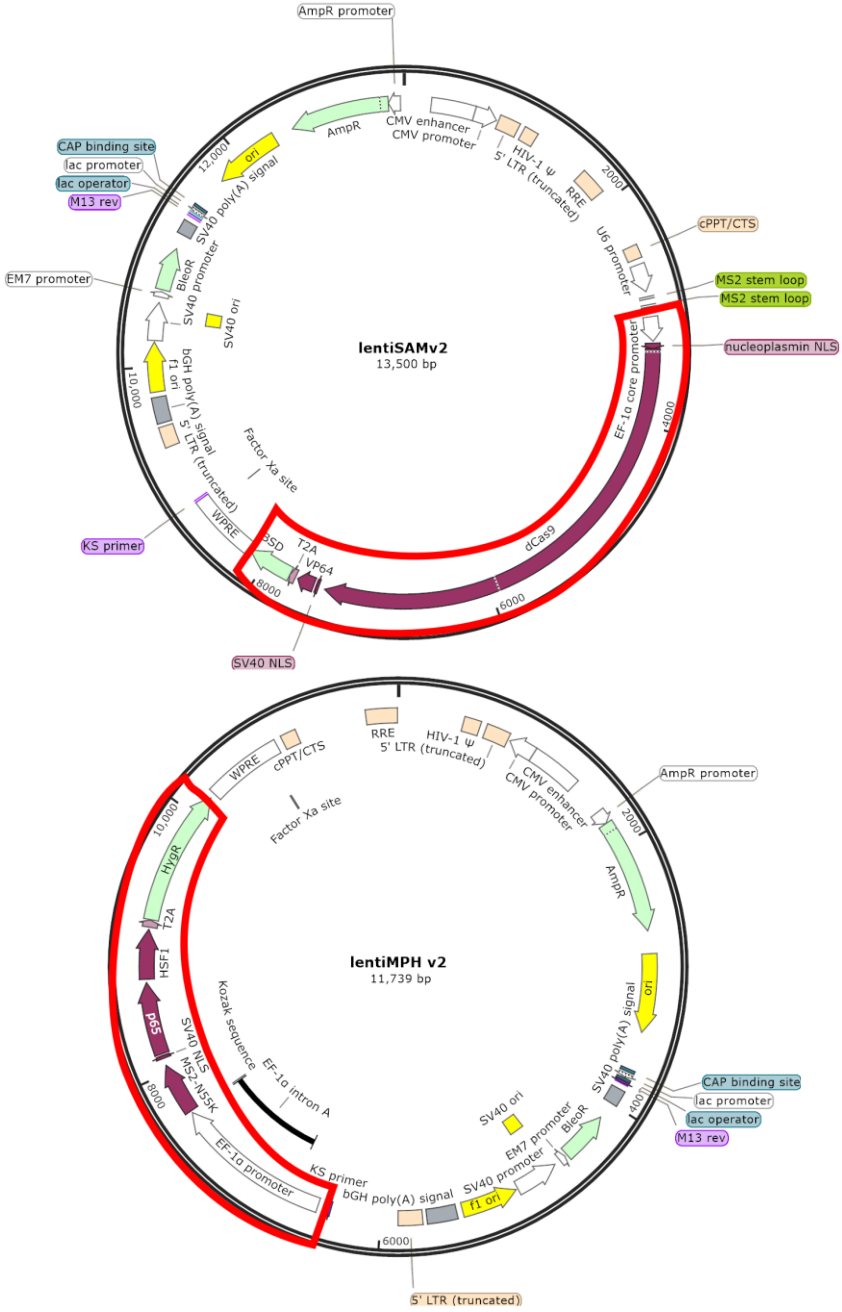
lentiSAMv2
13,500 bp
AmpR promoter
AmpR
CMV enhancer
CMV promoter
5' LTR (truncated)
HIV-1 Ψ
RRE
cPPT/CTS
U6 promoter
MS2 stem loop
MS2 stem loop
nucleoplasmin NLS
EF-1α core promoter
dCas9
VP64
T2A
BSD
WPRE
5' LTR (truncated)
bGH poly(A) signal
f1 ori
SV40 ori
SV40 promoter
BleoR
EM7 promoter
CAP binding site
lac promoter
lac operator
M13 rev
SV40 poly(A) signal
ori
Factor Xa site
KS primer
SV40 NLS
lentiMPH v2
11,739 bp
HygR
HSF1
p65
MS2-NS5K
Kozak sequence
EF-1α intron A
EF-1α promoter
KS primer
5' LTR (truncated)

Figure 1.1: Transcriptional activation by the SAMv2 system
(A) The SAMv2 vector codes for the dCas9 and sgRNA that has a MS2-binding stem-loop aptamer. The MPH vector codes for the activating domains HSF1 and P65, and the protein dimer MS2 that allows binding to the sgRNA. The activating domains and sgRNA-dCas9 form a complex via the MS2 and sgRNA stem-loop aptamer. The activating domain on the dCas9, VP64, act synergistically with the activating domains P65 and HSF1 to induce transcriptional upregulation of the gene targeted by the sgRNA spacer sequence. This figure is a modification of an illustration in Konermann et al., 2015. (B) Plasmid map of the SAMv2 vector (top) and MPH helper vector (bottom). The SAMv2 vector contains the blasticidin resistance gene (*BSD*) as a selectable marker, which is driven by the constitutive EF-1α promoter together with the sequences for dCas9 and the sgRNA (indicated in red). The MPH helper vector contains the hygromycin resistance gene (*HygR*) as a selectable marker, which is driven by the EF-1α promoter together with sequences for MS2, P65, and HSF1 (indicated in red).

1.5.2 Library amplification for NGS

As previously mentioned, the purpose of the PCR-amplification of gDNA harvested from enriched cells is to prepare the DNA (library) for NGS. In the SAMv2 system, the primers for the PCR are designed to amplify the spacer sequence to produce an amplicon of 270-280 base pairs (bp) in length (Joung et al., 2017). These primers also contain adapters that allow binding of the amplicons to the flow cell (the physical surface on which sequencing occurs) for Illumina's NGS. In addition, the reverse primers have unique barcodes that allow distinction between different samples during *in silico* analysis of sequencing results (Joung et al., 2017). There is a total of 8 different such barcodes, which means that the library from up to 8 different samples (or treatment groups) can be pooled together for a single sequencing run (Joung et al., 2017). Pooling samples is much more cost-efficient than sequencing each sample in individual runs.

1.5.3 Considerations for library sequencing

For the NGS, it is recommended by the developers of the SAMv2 system to have a minimum of 100 reads per each unique sgRNA in the library, which equates to about 7.0×10^6 reads (Joung et al., 2017). This means that during the NGS, each nucleotide is read 7×10^6 times to mitigate the occasional misreads caused by instrument error. There are many Illumina NGS instruments that can achieve this number of reads, including NextSeq, MiSeq, and HiSeq instruments (Joung et al., 2017). Any one of these instruments can be chosen according to availability, but the maximum number of reads available is ideal – due to the heavy use of time and resources involved in the CRISPRa screen, the costs of sequencing should be considered negligible. Another parameter to consider for NGS is the number of cycles, also known as read length. This refers to the length of the amplicon that is sequenced. Because only a part of the amplicon needs to be sequenced to recognize which sgRNA it corresponds to, the sequencing of its entire length is unnecessary. Longer read lengths allow more overlap with the reference sequence and thus lead to higher confidence, making it preferable for applications such as whole genome or whole exome sequencing. While a minimum read length of 80 bp is required for the purpose of determining library distribution in the SAMv2 system (Joung et al., 2017), higher read lengths are favorable to increase confidence in the sequenced data. Some instruments, like the HiSeq instrument, also have the option of paired-end sequencing. In this method, after the DNA is read from one end, it is read again in the opposite direction. In effect, this doubles the number of reads and improves confidence in the sequencing output.

1.5.4 Candidate gene analysis

The results of the NGS can be read using a computer language called Python (Joung et al., 2017). A script for determining library distribution is provided by the developers of the SAMv2 system (Supplementary Data 3 of Joung et al., 2017). This script gives read counts of each sgRNA in the library using the NGS output files. Using the read count information, statistical analysis must be done to determine the significance of the enrichment of candidate genes. A common analysis method is to use RNAi gene enrichment ranking (RIGER), which ranks sgRNAs according to the level of enrichment (or depletion in the case of LOF screens), and determines whether the sgRNAs that target each gene is biased towards the top of the ranked list using the

Kolmogorov-Smirnov statistic (Joung et al., 2017; König et al., 2007). Then, RIGER gives an enrichment score and relative ranking for each gene. In GOF screens such as those using the SAMv2 system, the genes that are ranked consistently high in RIGER analysis across biological replicates represent candidate genes.

2.0 Materials and Methods

2.1 Culture of OCI-AML3 and its derived cell lines

The OCI-AML3 cell line was purchased from Leibniz Institute DSMZ, German Collection of Microorganisms and Cell Cultures GmbH. Cells were cultured in minimum essential medium (MEM) α with 20% heat-inactivated (h.i.; 30 min at 50°C) fetal bovine serum (FBS). The ultra low attachment 6-well plate (Corning) was used for culture. Cells were passaged every 2-3 days to a density of approximately 5.0 x 10^5 cells/ml, 5 ml/well. The cell density was not allowed to exceed 2.0 x 10^6 cells/ml. Cell counting was done using Countess™ II Automated Cell Counter (ThermoFisher SCIENTIFIC).

The OCI-AML3 cell line expressing the MPH helper vector (single-resistant cells) was cultured using the same procedures, but the media contained 500 µg/ml of Hygromycin B (Santa Cruz Biotechnology). The OCI-AML3 cell line expressing both the MPH helper vector and the SAMv2 empty or library vector was cultured using the same procedures, but the media contained both 500 µg/ml of Hygromycin B and 5 µg/ml of Blasticidin S HCl (ThermoFisher SCIENTIFIC). For both variant cell lines, the antibiotic was always added during the passage and not during the making of the media.

Cells transduced with the MPH helper vector, or both the MPH helper vector and the SAMv2 empty vector, were selected with antibiotics and cryopreserved in -150°C. The freezing media was composed of 70% culture media, 20% FBS, and 10% dimethyl sulfoxide (DMSO). Cells expressing both the MPH helper vector and SAMv2 library were never cryopreserved or cultured for more than 2 days post-selection to avoid introducing bias in library distribution.

2.2 Amplification of the pooled SAMv2 library and MPH helper vector

The Human CRISPR 2-plasmid activation pooled library (SAMv2) was developed by Feng Zhang (Addgene #1000000078) and distributed by Addgene. The procedures for amplifying this library followed the instructions detailed in the corresponding publication (Joung et al., 2017). The library was delivered via electroporation at 50–100 ng/µl into Endura™ ElectroCompetent cells (Sigma-Aldrich) using the Gene Pulser Xcell™ Electroporation System (BioRad). Cells were diluted 10,000-fold and plated onto 5 large lysogeny broth (LB) agar plates (235-mm square bioassay dish) containing 100 µg/ml ampicillin. Plates were then incubated at 37°C for 12-14 hours. All colonies were harvested using two washes of 10 ml of LB medium per plate. Gathered cells were pooled and divided into a total of 3 pellets, and the plasmid library was extracted using HiSpeed® Plasmid Maxi Kit (Qiagen) on each pellet. Purity of the extracted library was measured using NanoDrop One Microvolume UV-Vis Spectrophotometer (ThermoFisher SCIENTIFIC).

The MPH helper vector (Addgene #89308) was amplified using One Shot™ Stbl3™ Chemically Competent *E. coli* cells (Thermofisher SCIENTIFIC), following the manufacturer's guidelines. After transformation, cells were plated onto LB agar ampicillin (100 µg/ml) plates and incubated for 12 hours in 37°C. A single colony was isolated and inoculated in 3 ml of LB broth containing ampicillin (100 µg/ml). About 6 hours later, 500 µl of this culture was mixed with 150 ml LB broth containing ampicillin (100 µg/ml) and cultured for 16-18 hours in 37°C. The cells were then pelleted and HiSpeed® Plasmid Midi Kit (Qiagen) was used to extract the plasmid.

2.3 Lentivirus production and titration

The human embryonic kidney (HEK) 293FT cell line was cultured until 100% confluency before transfection. For transfection, 13 µg of psPAX2, 9 µg of pMD2.G, 23 µg of vector DNA, and 250 µl of OptiMEM (ThermoFisher SCIENTIFIC) was mixed first for each T150 flask of HEK293FT. Separately, 3 ml of OptiMEM and 92 µl of Lipofectamine LTX (ThermoFisher SCIENTIFIC) were mixed and incubated for 4 min at room temperature. The first and second solutions were mixed dropwise and incubated for 20 min at room temperature. For each T150 flask of HEK293FT culture, the media was aspirated and replaced by 10 ml of the prepared solution. Approximately 12-18 hours later, 14 ml of additional media was added on top. The produced lentivirus was harvested in 60-66 hours via ultracentrifugation, and stored in -80°C.

Titration of the purified lentiviruses involved transduction at virus volumes ranging from 2.5 to 100 µl per 2.5 x 10^6 OCI-AML3 cells (wildtype), along with a non-transduced control condition. Cells transduced with the MPH helper vector were purified by selection with 400 µg/ml hygromycin (Santa Cruz Biotechnology) over 5 days, and cells transduced with the SAMv2 empty or library were purified by selection with 10 µg/ml blasticidin (ThermoFisher SCIENTIFIC) over 5 days (see the results section for optimization data). Note that these latter cells are wildtype OCI-AML3 transduced with only the SAMv2 vector solely for virus titration purposes and are not double-resistant cells (MPH+SAMv2). Selection for double resistant cells have different treatment conditions (refer to subsection 2.6).

2.5 Lentiviral transduction

The OCI-AML3 cells were passaged to 2.5 x 10^6 cells in 2 ml per well in a 6-well ULA plate. The media was supplemented with 8 µl/ml of polybrene (Sigma-Aldrich) and the virus was added (titrated volume). For lentiviral delivery of the MPH helper vector, a multiplicity of infection (MOI) of 70-100% was targeted, while lentiviral delivery of the SAMv2 empty or library targeted an MOI of 0.3 or less to prevent multiple vectors entering each cell. The titrated volumes to achieve the above MOIs were dependent on the batch of virus. After adding the virus, cells were centrifuged in the same 6-well ULA plate at 1200 rcf for 60 min. After centrifuging, cells were seen to form clumps on the outer areas of each well. These clumps of cells were dissociated by pipetting and cells were incubated in 37°C for 24 hours. Then, the cells were passaged to 5.0 x 10^5 cells/ml in culture media containing the appropriate selection antibiotic(s) (refer to next subsection).

2.6 Antibiotic selection for cells carrying the MPH helper vector or both the MPH and SAMv2 library/empty-control vectors

To select for cells carrying the MPH helper vector (single-resistant cells), cells were treated with hygromycin at a concentration of 400 µg/ml over 5 days (drug refreshed every 2 days during passage). To select for cells carrying both the MPH and SAMv2 library/empty-control vectors (double-resistant cells), cells were treated with blasticidin at a concentration of 5 µg/ml over 7 days, accompanied by hygromycin at a concentration of 400 µg/ml (both drugs refreshed every 2-3 days during passage). Cells were maintained at the same density as the wildtype's standard culture density (5.0 x 10^5 cells/ml to 2.0 x 10^6 cells/ml), for no longer than 2 days before transplant.

2.7 Transplant of OCI-AML3 and its derivative cell lines into mice

Mice of the NSG strain (Jackson Laboratory) were irradiated at 250 or 125 rad using a cesium-137 irradiator the day before transplant. Cells were resuspended in injection media (0.5% FBS in phosphate buffered saline (PBS)) at a density of 1.67 x 10^6 cells/ml. Cells were intravenously injected into the tail of each mouse, at a volume of 300 µl to achieve 5.0 x 10^5 cells.

In the subcutaneous injection method, cells were suspended in an ice-cold Matrigel (Corning)/PBS (1:1 ratio) mixture at a density of 2.5 x 10^7 cells/ml. The cell suspension was kept in ice until it was subcutaneously injected into the hind flak of mice, at a volume of 200 µl to achieve 5.0 x 10^6 cells per mouse. Mice were not irradiated in this transplant method.

2.8 Bone marrow aspirates

Mice were anesthetized with Isoflurane and 0.05 mg/kg of body weight of Buprenorphine was administered subcutaneously as a long-term analgesic. Hair from the knee area of each mouse was removed and disinfected using Proviodine detergent followed by 70% ethanol. An initial opening was created with a 27G ½" needle, followed by a 28G ½" needle to draw up approximately 5-10 µl of cells. Cells were dispensed into harvest media composed of 3% FBS and 1mM ethylenediaminetetraacetic acid (EDTA) (Sigma-Aldrich) in Iscove Modified Dulbecco Media (IMDM) (Gibco). The cell suspension was stored in 4°C for no longer than 2 hours. The cells were centrifuged and resuspended in ammonium chloride for about 10 min to lyse red blood cells before flow cytometry analysis for chimerism. Buprenorphine was administered again to each mouse in 24 hours.

2.9 Administration of AraC *in vivo*

Crystallized cytosine β-D-arabinofuranoside (Sigma-Aldrich) was dissolved in sterile PBS by sonication. The solution was administered to each mouse subcutaneously at a dose of 50 mg/kg of body weight. Supplementary saline solution was administered daily if mice showed any signs of deteriorating physical health (weight loss exceeding 10% or visual signs of poor condition).

2.10 Harvest of cells from mice

All bone marrow harvests that occurred at the mouse's endpoint came from the femur, tibia, and the iliac bone and crest of each mouse after euthanasia. Each bone was dislodged carefully and ground using a mortar and pestle into harvest media (described in subsection 2.8). The solution was strained and stored in 4°C for no longer than 2 hours. The cells were centrifuged and resuspended in ammonium chloride for about 10 min to lyse red blood cells before flow cytometry analysis for chimerism. Identical procedures were used for the cells harvested from the subcutaneous solid tumor, spleen, liver, and lungs, except they were ground directly on the strainer as opposed to the mortar.

2.11 Flow cytometry

To determine chimerism, cells were resuspended in 5% FBS + 2mM EDTA + PBS solution (PEF) and incubated for 15 min in 4°C with the conjugated antibody, hCD45-FITC (BD

Pharminogen), at a dilution of 1:100. UltraComp eBeads (Affymetrix eBioscience) were stained at the same dilution to be used for compensation analysis. Cells were then washed with PEF by centrifugation and resuspension. Live/dead staining was done using 7-aminoactinomycin D (7-AAD) (Beckman Coulter). Flow cytometry was performed with the BD™ LSR II flow cytometer and the BD FACS Diva software. Analysis of gathered data was done using FlowJo v10.6.1 (FlowJo, LLC).

To determine cell viability after antibiotic selection of OCI-AML3 and its derivative cell lines, cells were only stained with 7AAD.

3.0 Results

3.1 OCI-AML3 cell line was chosen for the CRISPRa screen

Primary tumor samples are ideal in screening studies for cancers because they approximate clinical conditions (Miller et al., 2017). However, because primary AML samples are vastly heterogenous, using them for a genome-wide screening has the drawback of introducing a significant variable; if primary AML samples are used, it would not be clear whether the candidate genes obtained from the screening are applicable only to the cell types in which they were expressed (Corces et al., 2016; Kumar, 2011; S. Li et al., 2016). The use of an AML cell line instead of a primary sample in the CRISPRa screening is therefore preferable because cell lines offer homogeneity, which eliminates the variable of cell type in the screening. Thus, an appropriate AML cell line was sought for use in the CRISPRa screening. Academic publications were searched based on three criteria: transducibility, to allow transduction of the lentivirus-based SAMv2 CRISPRa library and MPH helper vector; engraftability in mice, for the CRISPRa screening to be done *in vivo*; and susceptibility to AraC treatment, such that the cells not rescued by the library can be depleted.

A total of six cell lines that are widely used in AML research were considered, which were: OCI-AML3, HL-60, MOLM-14, MV4-11, U937 and KG1a. Pertinent information on each cell line are described below. For a condensed summary, please refer to Table 3.1.

- The HL-60 cell line was reported to be transducible (Jian et al., 2011; Pikman et al., 2016; Roddie et al., 2000), engraftable (Y.-L. Chen et al., 2015; Farge et al., 2017a; Saland et al., 2015), but not susceptible to AraC treatment *in vivo* (Farge et al., 2017a).
- The MOLM14 cell line was reported to be transducible with a lentiviral vector (Heydt et al., 2018; Wan et al., 2017), engraftable in NSG mice (Farge et al., 2017a; Green et al., 2015; Saland et al., 2015) but not susceptible to AraC treatment *in vivo* (Farge et al., 2017a).
- The MV4-11 cel line was reported to be transducible with a lentiviral vector (Caldarelli et al., 2013), engraftable in NSG mice (Farge et al., 2017a; Saland et al., 2015), but not susceptible to AraC treatment *in vivo* (Farge et al., 2017a).
- The U937 cell line was also reported to be transducible with high efficiency using a retroviral vector (He et al., 2018; Pikman et al., 2016; Roddie et al., 2000), engraftable in NSG and BALB/c (Bald Albino) mice (Farge et al., 2017a; He et al., 2018; Saland et al., 2015), and susceptible to AraC treatment *in vivo* (Farge et al., 2017a). However, although the U937 cell line is used in AML research and satisfies all the above requirements to be used in the CRISPRa screening, it was isolated from a patient with histiocytic lymphoma instead of AML despite its myeloma like features and was disregarded (Sundström & Nilsson, 1976).
- The OCI-AML3 cell line was reported to be transducible using a lentiviral vector (Balusu et al., 2011; Borthakur et al., 2015; Omsland et al., 2017; Xu et al., 2016), engraftble in in NSG and NOD/SCID mice (Balusu et al., 2011; Cho et al., 2015), and susceptible to AraC treatment *in vivo* (Balusu et al., 2011; Borthakur et al., 2015; Omsland et al., 2017; Xu et al., 2016). However, the OCI-AML3 cell line previously showed inconsistency in its engraftability in our lab.
- The KG1a cell line was reported to be transducible with high efficiency using a retroviral vector (Bierhuizen et al., 1999; Roddie et al., 2000; van Buul et al., 2003), engraftable in NSG mice (Farge et al., 2017a; Saland et al., 2015), and susceptible to AraC treatment *in vivo* (Farge et al., 2017a).

Based on the above information, the KG1a cell line was initially decided to be used for the CRISPRa screen. However, this cell line produced impractically low lentivirus transduction efficiency (Figure 3.1) and another cell line was sought. Note that in the case of KG1a, puromycin (optimized concentration of 2 μg/ml) was used instead of hygromycin because KG1a had resistance to hygromycin. A variant of the MPH vector that had a selectable marker for puromycin resistance was used. The other option for the cell line was to use the OCI-AML3 cell line, but this cell line had previously shown inconsistent chimerism and survival when transplanted in mice by our lab (unpublished). Upon resolving this issue in an engraftment experiment (discussed in next subsection), the OCI-AML3 cell line was chosen for the CRISPRa screen.

Table 3.1: Cell lines considered for the CRISPRa screen

AML cell line	Transducibility	Engraftability	Responsive to AraC
KG1a	Yielded poor transduction efficiency when tested with the SAMv2 library and empty vectors	Yes	Yes
U937 (lymphoblast cell line "with AML markers")	Yes	Yes	Yes
OCI-AML3	Yes	Yes	Yes
HL60	Yes	Yes	No
MOLM14	Yes	Yes	No
MV4-11	Yes	Yes	No

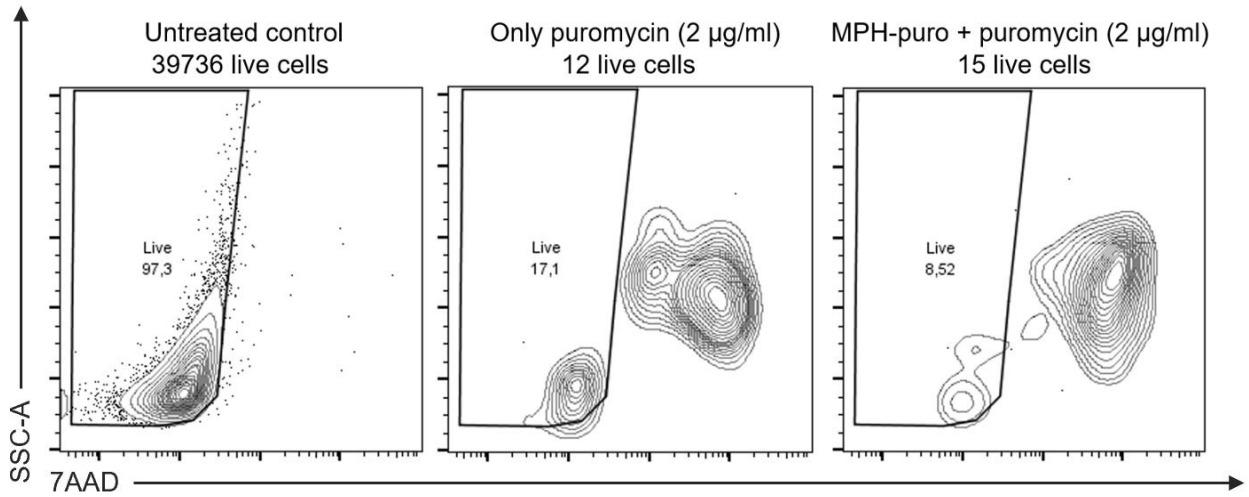

Figure 3.1: Attempts to transduce KG1a with the MPH vector yielded low efficiency.
Wildtype KG1a cells were transduced with the MPH helper vector that carries a selectable marker for resistance to puromycin (right). This variant of the MPH vector was used instead of the standard version that carries hygromycin resistance because KG1a had resistance to hygromycin. As controls, cells that were transduced but not treated with puromycin (left) and cells that were not transduced but treated with puromycin (middle) were included. After transduction, puromycin (lowest lethal dose, 2 µg/ml) was administered every 2 days over 4 days, followed by cell count and viability assessment using flow cytometry 24 hours after the last administration of the antibiotic.

3.2 Optimization of transplant route and cell dose for OCI-AML3 engraftment

Despite inconsistencies in chimerism previously found by our lab, the OCI-AML3 cell line was tested for engraftment in mice, but using conditions found in a publication that used the same cell line (Cho et al., 2015). The major difference in the method of transplant was the dose of irradiation preconditioning, which was 250 rad as opposed to our lab's standard practice of 315 rad. A total of 10 mice (NSG) were irradiated with 250 rad. Six mice were transplanted with 5.0 x 10^5 cells/mouse and four mice were transplanted with 1 x 10^6 cells/mouse, using IV injection through the tail. Mice were kept until ethical endpoint, euthanized, and cells were harvested from leg bone marrow to measure chimerism via flow cytometry. In parallel with the IV transplants, the subcutaneous transplant method using Matrigel was tested as backup in case the IV transplants yielded unfavorable results. Two mice were injected with 5.0 x 10^6 OCI-AML3 cells each, a dose that was decided based on literature sources that used the same cell line (Andresen et al., 2016; Floc'h et al., 2017). After becoming palpably large, the tumor size was measured every 2-3 days using a caliper. The mice were euthanized at ethical endpoint, and the tumors were extracted to determine chimerism by flow cytometry.

In the subcutaneous transplant method, both mice showed high chimerism (98.7 and 97.6%) (Figure 3.2A). In one mouse the tumor became palpably large around day 18 post-transplant, and day 26 post-transplant in the other (Figure 3.2B). Both mice survived until day 26 post-transplant (Figure 3.2C). In the IV transplant method, the two cell doses showed similar chimerism at endpoint: mice injected with 5.0 x 10^5 cells showed an average of about 50%, and mice injected with 1 x 10^6 cells showed an average of about 48% (Figure 3.3A). The two cell doses also showed similar survival periods: mice injected with 5.0 x 10^5 cells survived for an average of 25 days, and mice injected with 1 x 10^6 cells showed an average of 24 days (Figure 3.3B). Based on these data, IV injection of 5.0 x 10^5 cells per NSG mouse was determined to be suitable for the CRISPRa screen. The subcutaneous transplant method was deemed unfavorable because the IV transplant method is more clinically relevant and also showed reasonably high chimerism with consistent survival.

In the IV transplant method, In addition to harvesting from the leg bone marrow, cells were also harvested from other organs (ie. liver, lungs, and pancreas) in a mouse transplanted with 1 x 10^6 cells to determine if AML engraftment also occurs in these organs. Engraftment was found in each of these organs, with highest chimerism in the spleen, followed by liver, then lungs (Figure 3.4).

A

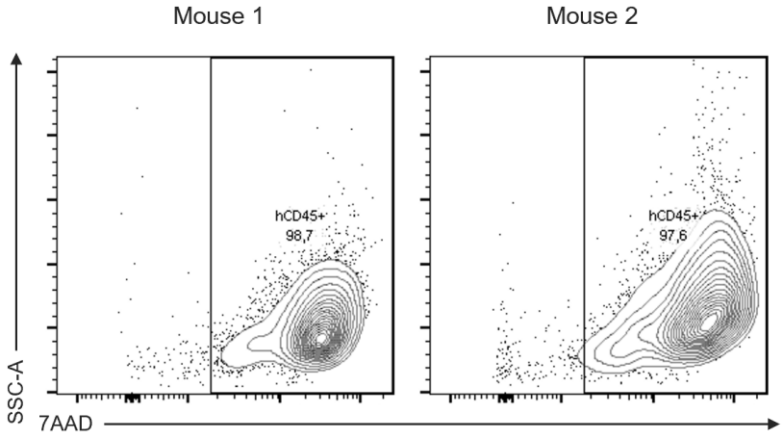
Mouse 1
Mouse 2
hCD45+
98,7
hCD45+
97,6
SSC-A
7AAD

B

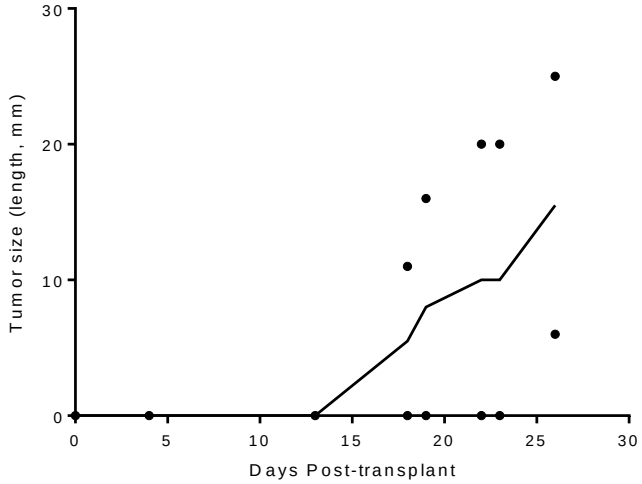
Tumor size (length, mm)
Days Post-transplant
0
10
20
30
0
5
10
15
20
25
30

C

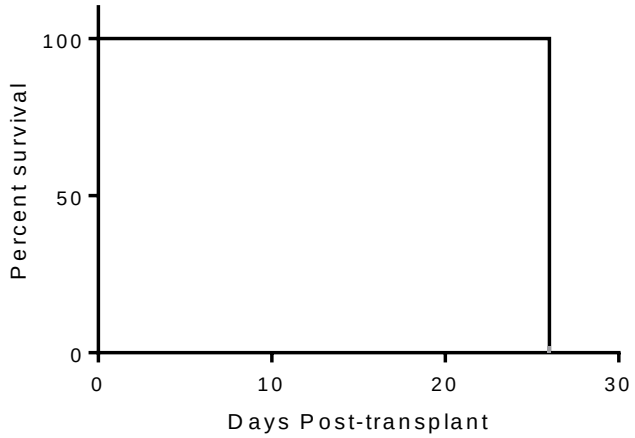
Percent survival
Days Post-transplant
0
50
100
0
10
20
30

Figure 3.2: Matrigel-mediated subcutaneous transplant of OCI-AML3 in mice led to high-chimerism tumors.
Two mice (NSG) were subcutaneously transplanted with OCI-AML3 (5×10^6 cells/mouse) using Matrigel as the vehicle. (A) Flow cytometry plots depicting chimerism (% $hCD45^+$) in the solid tumors formed. (B) Tumor sizes, as measured by a caliper every 2-3 days after becoming palpably large. (C) Kaplan Meier curves showing survival of the transplanted mice.

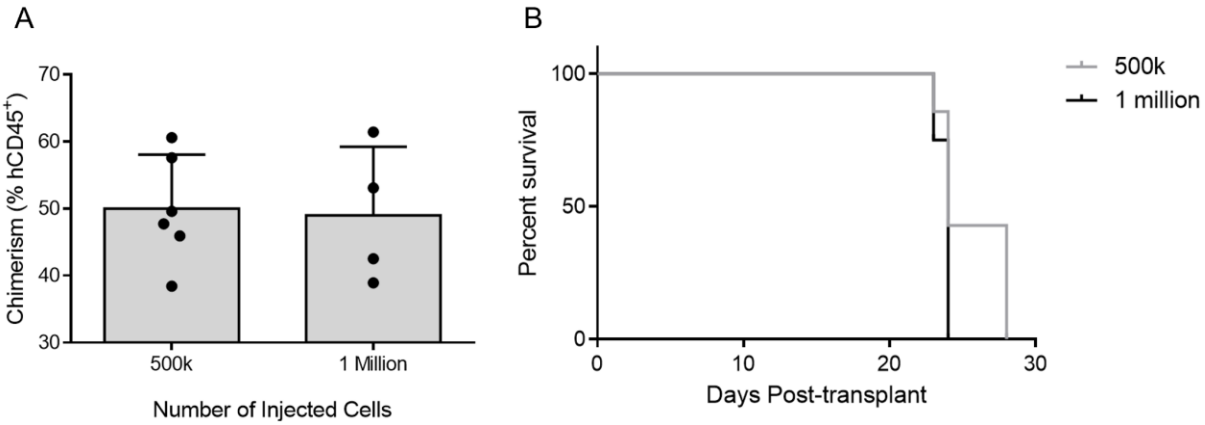

Figure 3.3: Intravenous injection of 5.0 x 10^5 OCI-AML3 cells/mouse is suitable for the CRISPRa screen.

Ten mice (NSG strain) were irradiated with 250 rad. Six mice were transplanted with 5.0 x 10^5 cells/mouse and four mice were transplanted with 1 x 10^6 cells/mouse, via intravenous injection. Mice were euthanized at ethical endpoint and chimerism was measured via flow cytometry. (A) Chimerism measured by % hCD45, and (B) Kaplan-Meier curves of mice injected with the two cell doses.

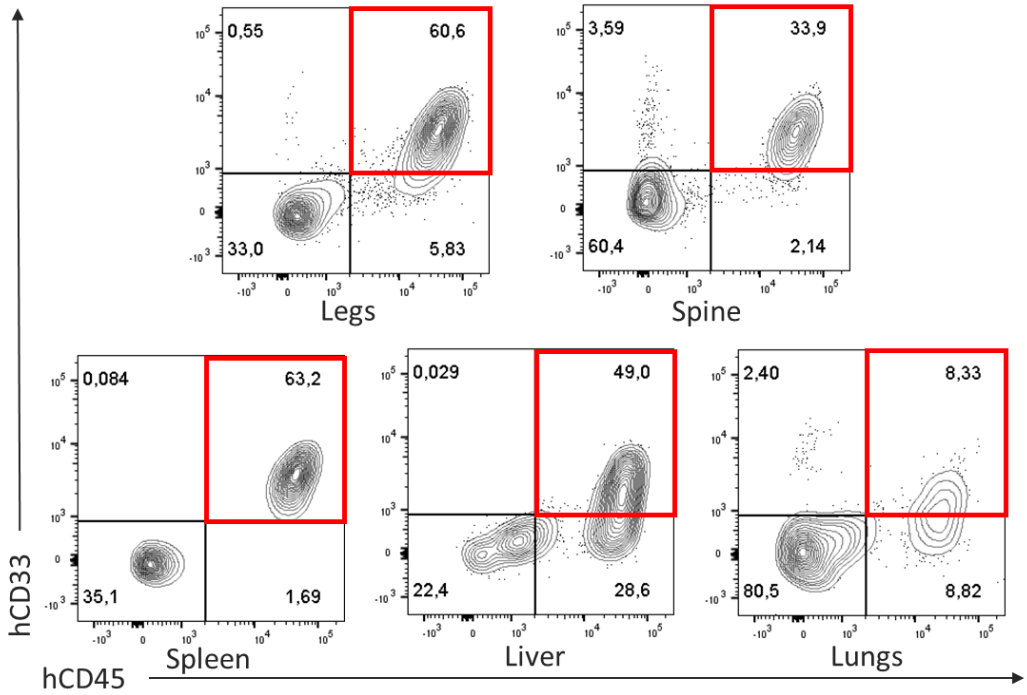

Figure 3.4: OCI-AML3 also engrafts in the spleen, liver, and lungs
An NSG mouse was irradiated with 250 rad and transplanted with 1 x 10^6 cells via intravenous injection. The mouse was euthanized at ethical endpoint and cells were harvested from the leg and spine bone marrow, spleen, liver, and lungs. Chimerism was measured via flow cytometry.

3.3 Optimization of post-transduction antibiotic selection conditions

To determine whether the selectable markers present in the MPH (hygromycin resistance, HygR) and SAMv2 library (blasticidin resistance, BSD) vectors can be used to select for transduced OCI-AML3 cells, various concentrations of the selection antibiotics were tested on OCI-AML3. The antibiotic, hygromycin or blasticidin, was administered every two days over 5 days, with viability assessment using 7AAD staining and flow cytometry on the fifth day. Concentrations of 100 μg/ml, 200 μg/ml, 400 μg/ml, and 800 μg/ml of hygromycin were tested. These treatments yielded 30.7%, 6.13%, 0.29%, and 0.23% surviving cells, respectively, relative to the untreated control (Figure 3.5A). The concentration of 400 μg/ml was thus found to be the ideal concentration to select for cells transduced with the MPH helper vector. For blasticidin, the selection antibiotic for the SAMv2 library and empty-control, concentrations of 2.5 μg/ml, 5 μg/ml, 10 μg/ml, and 20 μg/ml were tested. The treatments yielded 62.7%, 14.9%, 0.21%, and 1.56% surviving cells, respectively, relative to the untreated control (Figure 3.5B). The concentration of 10 μg/ml was therefore found to be ideal in selecting for cells transduced with the SAMv2 library or empty-control vector. Note, however, that this blasticidin selection condition cannot be used to select for cells carrying both the MPH helper vector and the SAMv2 library/empty-control ("double resistant cells), because this would have required the use of single resistant cells, not wildtype, for the kill curve. The optimized 10 μg/ml of blasticidin over 5 days was used only to titer the lentivirus carrying SAMv2 library/empty-control, using wildtype OCI-AML3.

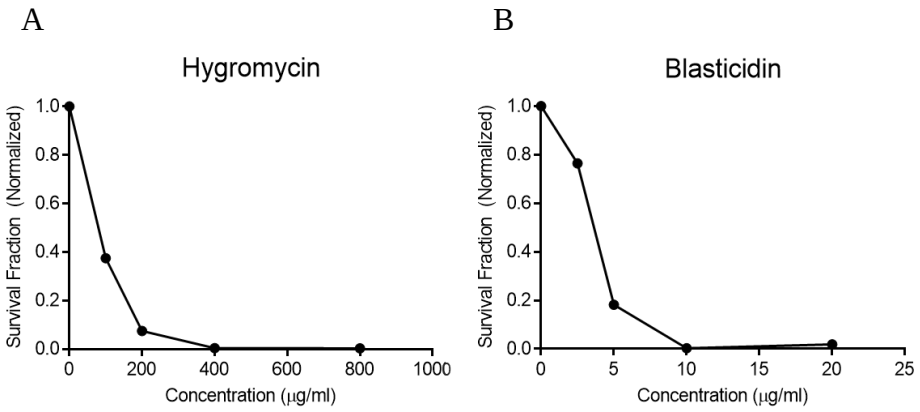

Figure 3.5: Optimized antibiotic concentration and treatment duration used to select for wildtype OCI-AML3 transduced with either MPH or SAMv2 library/empty-control vector. Wildtype OCI-AML3 cells were transduced with either the MPH helper vector or the SAMv2 empty-control vector. Cells transduced with the former were treated with hygromycin, and cells transduced with the latter were treated with blasticidin. The respective antibiotic was administered every 2 days over 4 days, followed by viability assessment using flow cytometry 24 hours after the last administration of the antibiotic. (A) Cells treated with hygromycin at concentrations of 100 μg/ml, 200 μg/ml, 400 μg/ml, and 800 μg/ml. (B) Cells treated with blasticidin at concentrations of 2.5 μg/ml, 5 μg/ml, 10 μg/ml, and 20 μg/ml.

To determine blasticidin selection conditions that can be used to select for double-resistant OCI-AML3 carrying both MPH and SAMv2 empty-control vectors (*HygR+BSD*), single resistant OCI-AML3 cells (*HygR*) were administered blasticidin concentrations of 2.5 μg/ml, 5 μg/ml, 7.5 μg/ml, and 10 μg/ml, with an untreated control on the side (Figure 3.6A). Double resistant OCI-AML3 cells were treated in parallel to confirm that these cells survive the optimized selection concentration (Figure 3.6B). Both the treatments of single-resistant and double-resistant cells included 400 μg/ml of hygromycin. The antibiotics were refreshed at every passage (every 2-3 days). Total cells were counted, and viability was assessed by 7AAD staining followed by flow cytometry. Single-resistant cells were found to be depleted when treated with blasticidin at a concentration of 5 μg/ml over 7 days. Double-resistant cells were confirmed to survive these selection conditions. In parallel with the above kill curves, supplemental controls were added. Wildtype OCI-AML3 was also treated with blasticidin as a positive control to ensure that the antibiotic batch in use was effective (Figure 3.6C). Also, single-resistant cells transduced with another vector with the same blasticidin resistance gene (*DMAP1-BSD*, Addgene) was also treated with blasticidin to ensure that any potential lack of resistance in double-resistant cells is not due to the SAMv2 plasmid backbone (Figure 3.6D).

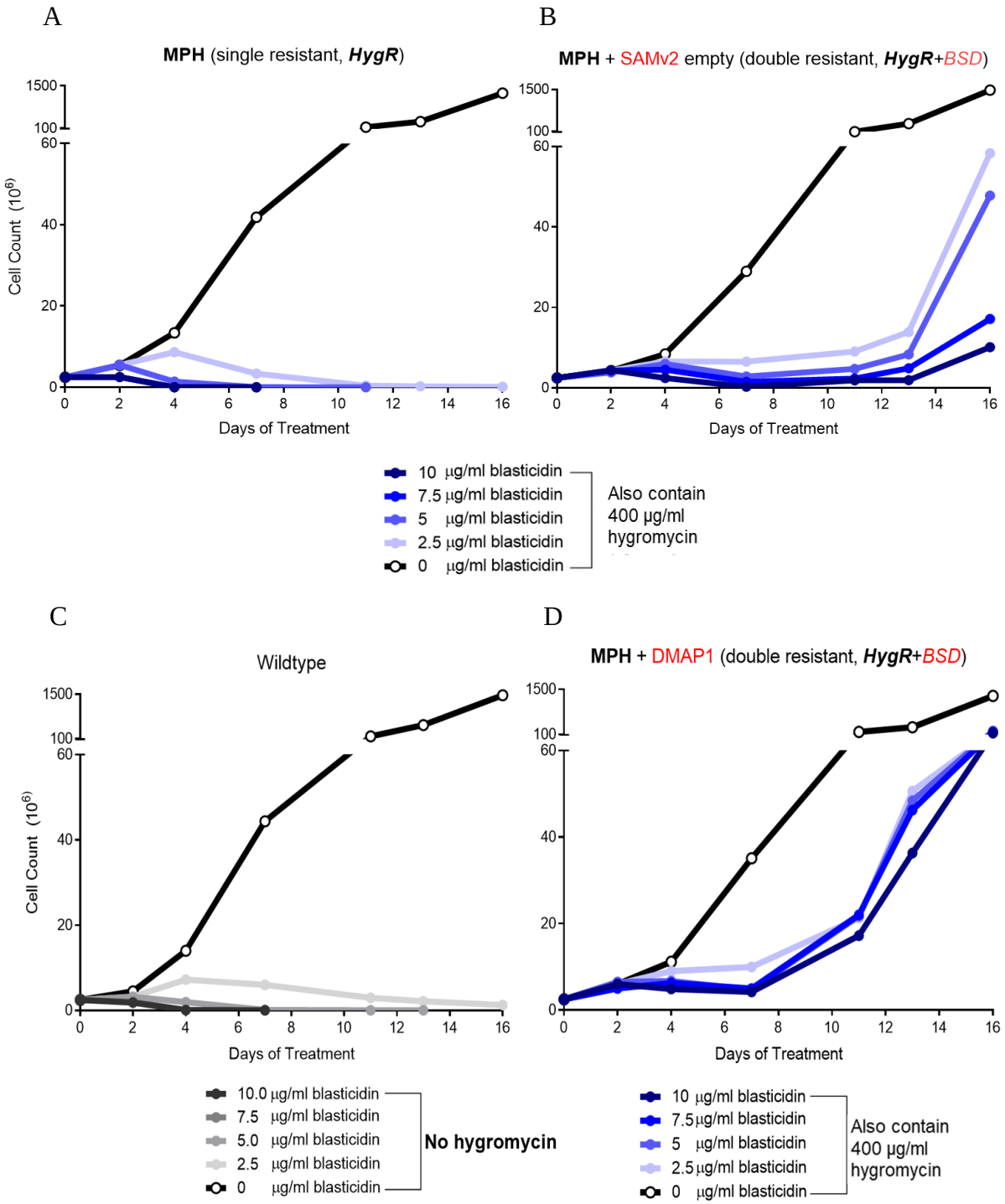
A
MPH (single resistant, HygR)
B
MPH + SAMv2 empty (double resistant, HygR+BSD)
Cell Count (10^6)
Days of Treatment
10 µg/ml blasticidin
7.5 µg/ml blasticidin
5 µg/ml blasticidin
2.5 µg/ml blasticidin
0 µg/ml blasticidin
Also contain 400 µg/ml hygromycin
C
Wildtype
D
MPH + DMAP1 (double resistant, HygR+BSD)
10.0 µg/ml blasticidin
7.5 µg/ml blasticidin
5.0 µg/ml blasticidin
2.5 µg/ml blasticidin
0 µg/ml blasticidin
No hygromycin

Figure 3.6: Optimized blasticidin concentration and treatment duration to select for double-resistant OCI-AML3 (carrying both MPH and SAMv2 library/empty-control vectors)
Single resistant and double resistant OCI-AML3 cells were treated with hygromycin and varying concentrations of blasticidin. Wildtype and a variant double-resistant OCI-AML3 (HygR + *BSD-DAMP1)* cells were treated with blasticidin as supplemental controls. Antibiotics were refreshed every 2-3 days up to 16 days. Cells were counted and viability was assessed via flow cytometry every two days. (A) Single-resistant cells treated with hygromycin (400 μg/ml) and blasticidin (2.5 μg/ml, 5 μg/ml, 7.5 μg/ml, and 10 μg/ml). (B) Double-resistant cells carrying MPH and SAMv2 treated with hygromycin (400 μg/ml) and blasticidin (2.5 μg/ml, 5 μg/ml, 7.5 μg/ml, and 10 μg/ml). (C) Wildtype OCI-AML3 was treated with blasticidin to ensure that the antibiotic batch in use was effective. Identifical concentrations of blasticidin were tested (2.5 μg/ml, 5 μg/ml, 7.5 μg/ml, and 10 μg/ml) over 16 days. No hygromycin was added. (D) A variant double-resistant OCI-AML3 cell line was produced by transducing single-resistant cells with *DMAP1-BSD*. These cells were then treated with hygromycin (400 μg/ml) and blasticidin (2.5 μg/ml, 5 μg/ml, 7.5 μg/ml, and 10 μg/ml) over 16 days.

3.4 Optimization of pre-conditioning irradiation dose, and kinetic profiling of double-resistant OCI-AML3 cells *in vivo*

In subsection 3.2, mice were irradiated at a dose of 250 rad to test engraftment of OCI-AML3. This dose was based on a literature source (Cho et al., 2015) that used the same strain of mouse (NSG) and cell line. However, when combined with *in vivo* AraC treatment, all mice died 2-3 days after the end of treatment (Figure 3.7). The goal of this experiment was to observe the change in chimerism when AraC is administered *in vivo*. A total of 10 NSGs were irradiated at 250 rad and transplanted with 5 x 10^5 cells/mouse the next day, as per optimization in subsection 3.2. The cells were double-resistant cells carrying MPH and SAMv2 empty-control vectors. Engraftment was confirmed by bone marrow aspirates a week later. Following a literature source (Boyd et al., 2018) that involved *in vivo* AraC treatment of AML patient derived xenografts (PDX), mice (5 of 10) were treated with AraC 8 days post-transplant at a dose of 50 mg/kg of body weight, 5 shots interspaced by 24 hours. About 2-3 days after the last shot, all 5 mice either died unexpectedly or reached the ethical endpoint. This result was consistent over two attempts of the experiment. It was hypothesized that the combined harsh insults of irradiation and chemotherapy led to the death of mice, and a lower irradiation dose was sought.

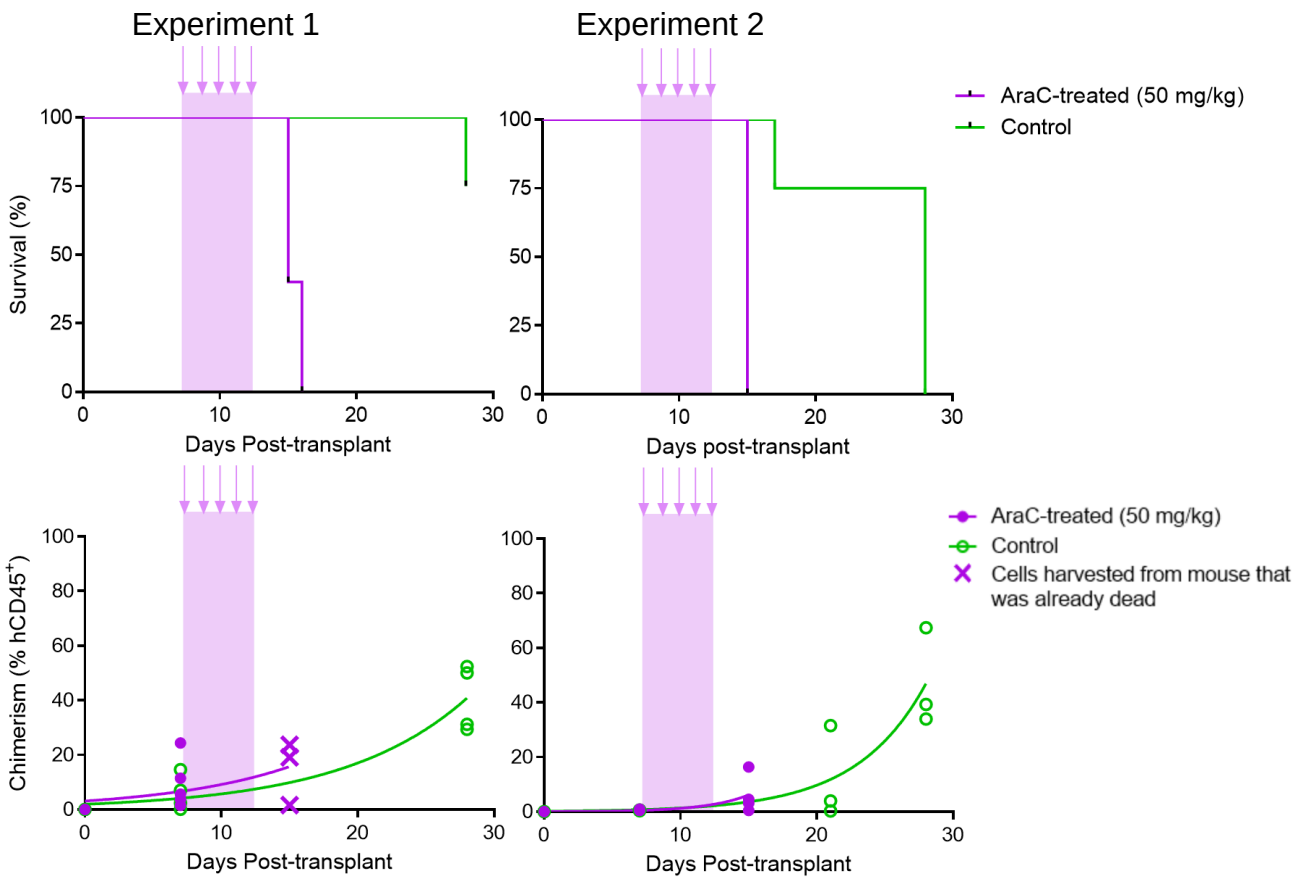

Figure 3.7: Combination of 250 rad and *in vivo* AraC treatment consistently led to early death of mice transplanted with double-resistant OCI-AML3.

This experiment was performed two times. A total of 10 NSG mice (8 in experiment 2) were irradiated with 250 rad and transplanted with 5 x 10^5 cells/mouse the next day. The cells were double-resistant cells carrying the MPH and SAMv2 empty-control vectors. Seven days post-transplant, engraftment was confirmed using bone marrow aspirates. The following day, 5 of the mice were treated with AraC (50 mg/kg of body weight), administered 5 times in 24 hr intervals. Time period shaded in purple represent AraC treatment, with arrows above representing the 5 individual AraC administrations. In some cases, cells had to be harvested from mice that were already dead, which shows falsely elevated chimerism.

Previous work from our lab (unpublished) suggested that irradiation at the "half dose" markedly reduces radiation-associated mortality. This experiment involved irradiation of newborn NOD/SCID mice at 100 rad, which is standard practice for this age (Risueño et al., 2011), followed by transplantation with primary AML cells. At about 6 weeks after the first irradiation, mice were given various irradiation doses ranging from 150 to 350, where 350 rad was the standard dose at that age (Burger et al., 2007). The mice irradiated with 150 and 200 rad were found to have no mortalities following the second irradiation, suggesting that reducing the irradiation dose by half may be a good starting point in optimizing the working irradiation dose for the CRISPRa screen. Based on this previous finding, the half irradiation dose was tested in combination with AraC to determine if it improves mouse survival post-chemotherapy. A total of 9 NSGs were irradiated with 125 rad and transplanted with 5 x 10^5 cells/mouse the next day. Again, these were double-resistant cells carrying the MPH and SAMv2 empty-control vectors. Engraftment was confirmed by bone marrow aspirates a week later (~1% chimerism), and AraC was administered at the same dose and schedule as before to 5 out of the 9 mice. Out of the 5 treated mice, 2 mice survived for as long as the control mice, while the rest died a few days following chemotherapy (Figure 3.8A). Chimerism of each mouse was tracked by bone marrow aspirates, or, if the mouse was at its endpoint, euthanasia. On average, the chimerism of AraC-treated mice were generally lower than that of the untreated control group at endpoint (approximately 42% and 65%, respectively) (Figure 3.8B and C). While 2 out of 5 treated mice surviving the AraC-treatment may seem like an impractically low survival rate, several measures can be taken to improve the survival rate during the CRISPRa screen: the bone marrow aspirate 1 day prior to AraC treatment can be omitted, as this is unnecessary during the actual screen; mice can be placed on the heat pad since the start of AraC treatment (this is usually done only when the mice start to appear sick); and lastly, the mice can be given daily supplemental saline injections after AraC treatment to improve general health.

In both the treated and untreated control groups, mice survived for about 28 days post-transplant before reaching ethical endpoint. This ethical endpoint at 28 days was often characterized by hind-limb paralysis, as is common in xenografts of this cell line (Xu et al., 2016). To capture the dominant clones that contribute to AML relapse with minimal noise, the harvest should take place at the latest timepoint possible, which would be 28 days post-transplant.

A

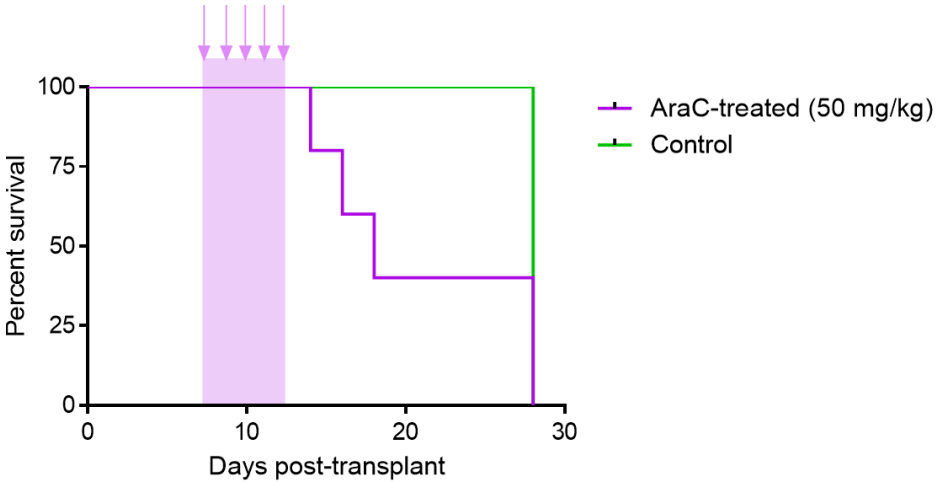
Percent survival
100
75
50
25
0
0
10
20
30
Days post-transplant
AraC-treated (50 mg/kg)
Control

B

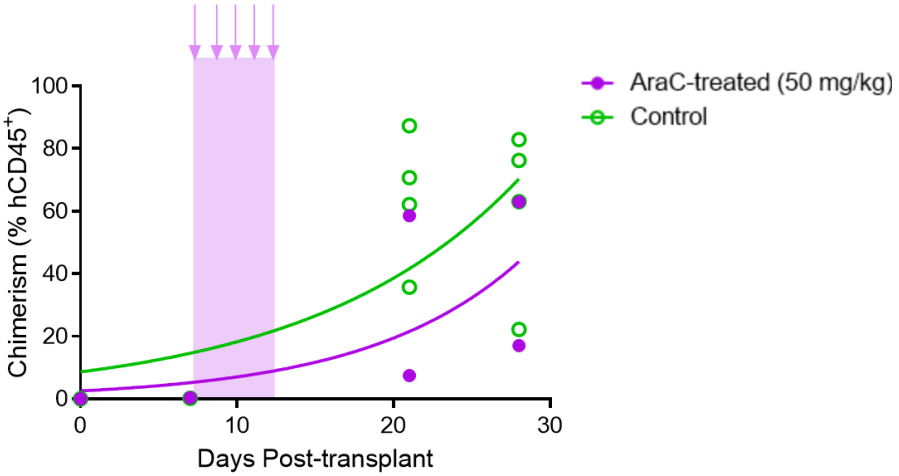
Chimerism (% hCD45+)
100
80
60
40
20
0
0
10
20
30
Days Post-transplant
AraC-treated (50 mg/kg)
Control

C

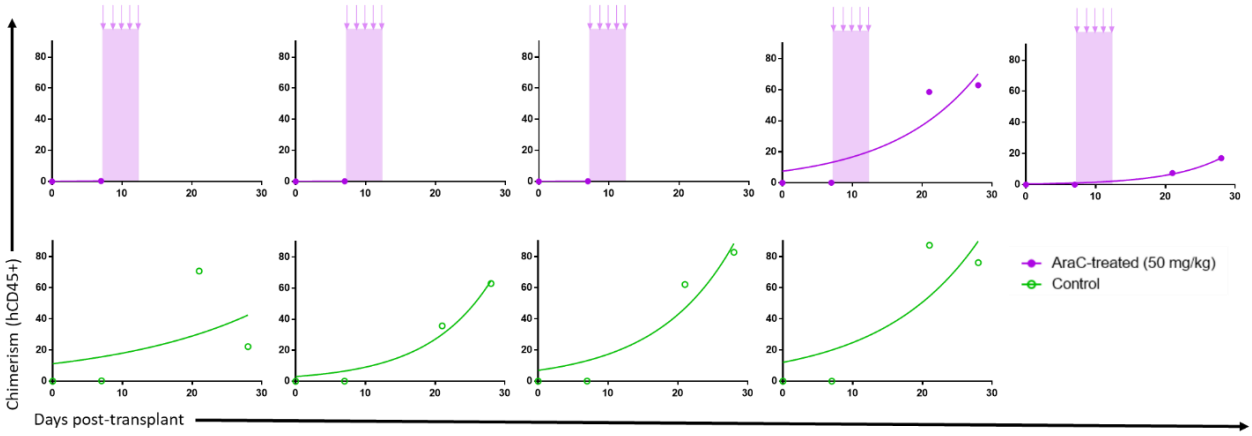
Chimerism (hCD45+)
Days post-transplant
AraC-treated (50 mg/kg)
Control

Figure 3.8: Use of 125 rad pre-conditioning allowed survival of transplanted mice following AraC treatment

A total of 9 NSG mice were irradiated with the "half dose," 125 rad, and transplanted with 5 x 10^5 cells/mouse the next day. The cells were double-resistant cells carrying the MPH and SAMv2 empty-control vectors. Seven days post-transplant, engraftment was confirmed using bone marrow aspirates. The following day, 5 of the mice were treated with AraC (50 mg/kg of body weight), administered 5 times in 24 hr intervals. Time period shaded in purple represent AraC treatment, with arrows above representing the 5 individual AraC administrations. (A) Kaplan-Meier curves of mice in the experimental (purple) and control (green) groups. (B) Compiled chimerism in each of the two groups. (C) Chimerism in individual mice shown separately.

To summarize, the results of this experiment showed that:

- chimerism of mice just before AraC-treatment is ~1%
- the 125 rad dose of irradiation allow survival of mice after AraC treatment
- chimerism of AraC-treated mice are lower on average than that of untreated mice
- mice survive for about 28 days before reaching ethical endpoint.

These findings, along with optimized parameters reported in previous subsections, were used to determine the number of mice required for a single replicate of the CRISPRa (described in the next subsection).

3.5 Determination of the total number of mice required for one replicate of CRISPRa screen

The number of mice required for each replicate of the CRISPRa screen depends on the decided coverage. The coverage refers to the number of cells per each unique sgRNA in the library. Note that the term, "coverage," is also often used to describe the number of unique reads for a given nucleotide in the amplicon. To avoid confusion, the latter meaning of this term is written as "number of reads" in this thesis. The coverage (number of cells per unique sgRNA) must be met at the point of applying the selection pressure and at the point of harvest for sequencing (Joung et al., 2017). A library of 100 unique sgRNAs with 10x coverage, for example, would mean a total of 1000 cells at the points of selection and harvest for sequencing. Theoretically, the higher the coverage the higher the statistic confidence in the results, but the maximum coverage is always limited by practicality. For the purpose of this CRISPRa screen, a coverage of 100x was decided because a higher coverage would lead to an impractical number of mice in terms of costs.

For a summary of the required number of mice for 1 replicate of the CRISPRa screen, please refer to Table 3.2 below. For the SAMv2 library, which has a total of 70,290 unique sgRNAs, 100x coverage corresponds to about 7.0×10^6 cells that must be present at both the time of AraC treatment (8 days post-transplant) and at harvest (endpoint, 28 days post-transplant). However, because the chimerism is always much higher at the endpoint, the time of AraC treatment was the focus when calculating the required number of mice. Previous work from our lab showed that after irradiation (315 rad) of NSGs, the bone marrow cellularity stays constant for a few weeks while the chimerism increases. Combining this information with the average cell count from the leg bone marrow obtained at the endpoint of the kinetic profiling experiment (1.5×10^7 cells per mouse), it was estimated that the cell count at the time of AraC treatment was approximately the same. Note, however, that because this is an approximation, a parallel or preliminary experiment should be run in addition to the CRISPRa screen where one or more mice are euthanized at this timepoint to determine the accurate total bone marrow cellularity. Next, to determine the number of engrafted cells present in each mouse at this time, the chimerism determined by bone marrow aspirate (subsection 3.4) was used. The bone marrow aspirate, taken 1 day before AraC treatment, showed ~1% chimerism. Combining this information with the bone marrow cellularity at this time, gives 1.5×10^5 engrafted cells per mouse. The cellularity in the leg bone marrow is about 20% of the mouse's total bone marrow (Colvin et al., 2004). If, during the CRISPRa screen, bone marrow is also harvested from the rest of the mouse (ie. spine, skull, ribs, etc.), a total of 7.5×10^5 engrafted cells would be present the day before AraC treatment. To determine the required number of mice screening, the required number of cells for 100x coverage of the library (7.0×10^6) was divided by the number of engrafted cells per mouse the day before AraC treatment (7.5×10^5). From this calculation, approximately 10 mice were found to be required for each group in the screen. This

number must be doubled to account for an untreated control group and a treated experimental group. In addition, 3 mice will be added to the experimental group and 2 mice will be added to the untreated control group for a total of 25 mice for 1 replicate of the CRISPRa screen.

Table 3.2: Calculation of the total number of mice required for 1 replicate of screening

Approximate leg bone marrow cell count at AraC treatment (~20% of whole BM)	= 1.5×10^7 cells/mouse
Estimated total bone marrow cell count at AraC treatment ($7.5 \times 10^7 \times 5$)	= 7.5×10^7 cells/mouse
Chimerism prior to AraC is ~1%	= 7.5×10^5 cells/mouse
Complete library of sgRNAs in the SAMv2 system	= 7.0×10^4 sgRNAs
100x coverage per sgRNA ($7.2 \times 10^4 \times 100$)	= 7.0×10^6 cells required
7.0×10^6 cells required / 7.5×10^5 cells per mouse	≈ 10 mice
(10 mice for experimental group + 3 extra) + (10 mice for control group + 2 extra)	= 25 mice total

3.6 Summary of optimized *in vitro* and *in vivo* parameters for the CRISPRa screen

Figure 3.9 and Figure 3.10 in the following pages summarize the *in vitro* and *in vivo* procedures for the CRISPRa screen, respectively. These summarized procedures include the optimized parameters reported in subsections 3.1 to 3.5.

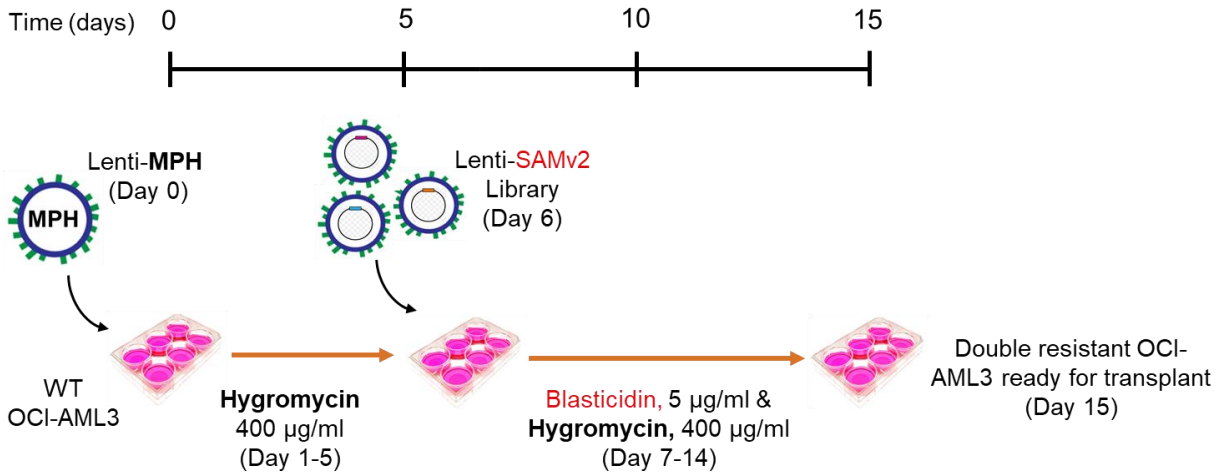

Figure 3.9: Workflow of *in vitro* preparation of double resistant cells for the CRISPRa screen. To produce single-resistant cells, wildtype OCI-AML3 is transduced with lenti-MPH and selected with hygromycin (400 µg/ml) over 5 days, passaged every 2 days. Single-resistant cells are then transduced with the SAMv2 library (MOI ≤ 0.3) and selected with blasticidin (5 µg/ml) and hygromycin (400 µg/ml) over 7 days, passaged every 2-3 days (a frozen stock of single-resistant cells can also be used). The double-resistant cells are then ready for transplant into mice.

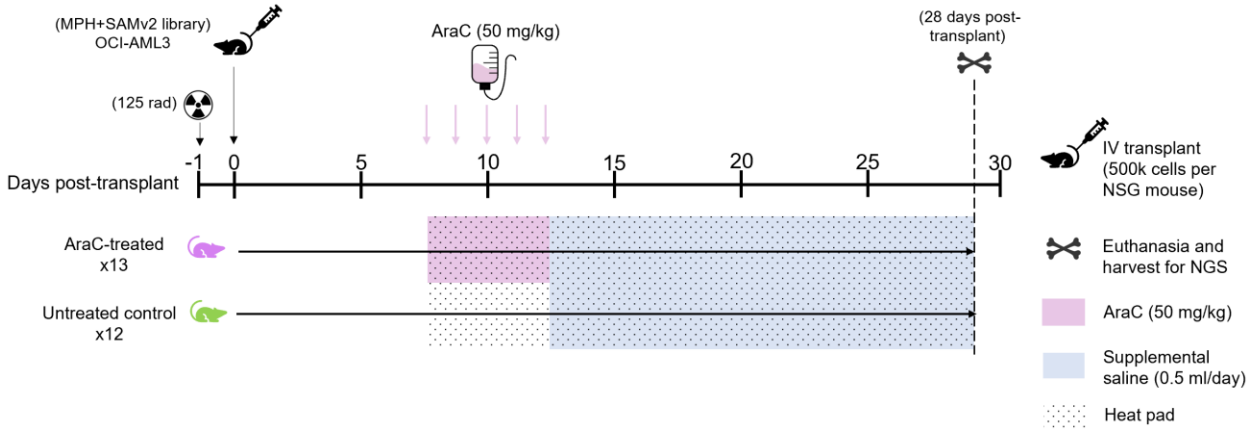

Figure 3.10. Summary of *in vivo* procedures for CRISPRa screen.
A total of 25 NSG mice will be preconditioned with 125 rad of irradiation. The next day, these mice will be transplanted with 5 x 10^5 double-resistant OCI-AML3 cells per mouse by IV injection. Starting from day 8 post-transplant, 13 mice in the experimental group will be administered AraC (50 mg/kg of body weight) subcutaneously, 5 times in 24-hour intervals. All mice will be placed on the heat pad starting on the first day of AraC-treatment. Starting on the first day after AraC-treatment, all mice will be given supplemental saline injections everyday until day 28 post-transplant. At this day, all mice will be euthanized so that all cells in the bone marrow can be harvested in preparation for submission for NGS.

3.7 Post-*in* vivo: procedures for library amplification and NGS

The genomic DNA of the mice should be harvested using the Quick-gDNA MidiPrep (Zymo Research) (Joung et al., 2017). Before submission for NGS, the harvested DNA must be PCR-amplified in the region of the incorporated spacer sequence. This PCR must use a high-fidelity DNA polymerase, such as the KAPA HiFi HotStart ReadyMix, 2× (Kapa Biosystems) (Joung et al., 2017). After PCR, the product must be purified using the QIAquick PCR Purification Kit (Qiagen, cat. no. 28104) (Joung et al., 2017). Specific primers that target the spacer sequences (Joung et al., 2017) are shown in Table 3.3. These primers include Illumina adapter sequences. All 10 NGS-Lib-Fwd primers are required for amplification of the library for NGS, while the NGS-Lib-SAM-Rev primers contain unique barcodes (indicated in bold) that can be used to distinguish between treatment groups within the submitted pooled sample (Joung et al., 2017). There is also the option of using a unique barcode for each mouse, which is discussed in more detail in the Discussion section.

Table 3.3: Primers for the amplification of the SAMv2 library before submission for NGS

Primer label	Primer sequence (5'-3')
NGS-Lib-Fwd-1	AATGATACGGCGACCACCGAGATCTACACTCTTTCCCTACACGACGCTCTTCCGA TCTTAAGTAGAGGCTTTATATATCTTGTGGAAAGGACGAAACACC
NGS-Lib-Fwd-2	AATGATACGGCGACCACCGAGATCTACACTCTTTCCCTACACGACGCTCTTCCGA TCTATCATGCTTAGCTTTATATATCTTGTGGAAAGGACGAAACACC
NGS-Lib-Fwd-3	AATGATACGGCGACCACCGAGATCTACACTCTTTCCCTACACGACGCTCTTCCGA TCTGATGCACATCTGCTTTATATATCTTGTGGAAAGGACGAAACACC
NGS-Lib-Fwd-4	AATGATACGGCGACCACCGAGATCTACACTCTTTCCCTACACGACGCTCTTCCGA TCTCGATTGCTCGACGCTTTATATATCTTGTGGAAAGGACGAAACACC
NGS-Lib-Fwd-5	AATGATACGGCGACCACCGAGATCTACACTCTTTCCCTACACGACGCTCTTCCGA TCTTCGATAGCAATTCGCTTTATATATCTTGTGGAAAGGACGAAACACC
NGS-Lib-Fwd-6	AATGATACGGCGACCACCGAGATCTACACTCTTTCCCTACACGACGCTCTTCCGA TCTATCGATAGTTGCTTGCTTTATATATCTTGTGGAAAGGACGAAACACC
NGS-Lib-Fwd-7	AATGATACGGCGACCACCGAGATCTACACTCTTTCCCTACACGACGCTCTTCCGA TCTGATCGATCCAGTTAGGCTTTATATATCTTGTGGAAAGGACGAAACACC
NGS-Lib-Fwd-8	AATGATACGGCGACCACCGAGATCTACACTCTTTCCCTACACGACGCTCTTCCGA TCTCGATCGATTTGAGCCTGCTTTATATATCTTGTGGAAAGGACGAAACACC
NGS-Lib-Fwd-9	AATGATACGGCGACCACCGAGATCTACACTCTTTCCCTACACGACGCTCTTCCGA TCTACGATCGATACACGATCGCTTTATATATCTTGTGGAAAGGACGAAACACC
NGS-Lib-Fwd-10	AATGATACGGCGACCACCGAGATCTACACTCTTTCCCTACACGACGCTCTTCCGA TCTTACGATCGATGGTCCAGAGCTTTATATATCTTGTGGAAAGGACGAAACACC
NGS-Lib-SAM-Rev-1	CAAGCAGAAGACGGCATACGAGAT**TCGCCTTG**GTGACTGGAGTTCAGACGTGT GCTCTTCCGATCTGCCAAGTTGATAACGGACTAGCCTT
NGS-Lib-SAM-Rev-2	CAAGCAGAAGACGGCATACGAGAT**ATAGCGTC**GTGACTGGAGTTCAGACGTGT GCTCTTCCGATCTGCCAAGTTGATAACGGACTAGCCTT
NGS-Lib-SAM-Rev-3	CAAGCAGAAGACGGCATACGAGAT**GAAGAAGT**GTGACTGGAGTTCAGACGTGT GCTCTTCCGATCTGCCAAGTTGATAACGGACTAGCCTT
NGS-Lib-SAM-Rev-4	CAAGCAGAAGACGGCATACGAGAT**ATTCTAGG**GTGACTGGAGTTCAGACGTGT GCTCTTCCGATCTGCCAAGTTGATAACGGACTAGCCTT
NGS-Lib-SAM-Rev-5	CAAGCAGAAGACGGCATACGAGAT**CGTTACCA**GTGACTGGAGTTCAGACGTGT GCTCTTCCGATCTGCCAAGTTGATAACGGACTAGCCTT
NGS-Lib-SAM-Rev-6	CAAGCAGAAGACGGCATACGAGAT**GTCTGATG**GTGACTGGAGTTCAGACGTGT GCTCTTCCGATCTGCCAAGTTGATAACGGACTAGCCTT
NGS-Lib-SAM-Rev-7	CAAGCAGAAGACGGCATACGAGAT**TTACGCAC**GTGACTGGAGTTCAGACGTGT GCTCTTCCGATCTGCCAAGTTGATAACGGACTAGCCTT
NGS-Lib-SAM-Rev-8	CAAGCAGAAGACGGCATACGAGAT**TTGAATAG**GTGACTGGAGTTCAGACGTGT GCTCTTCCGATCTGCCAAGTTGATAACGGACTAGCCTT

The library should be PCR-amplified using the parameters detailed in Table 3.4 below (Joung et al., 2017). The amplicon produced should be 270-280 bp. Before using the primers for the harvested library, they should be tested using the SAMv2 library DNA, extracted during the earlier maxiprep, in agarose gel electrophoresis to confirm the 270-280 bp amplicon size.

Table 3.4: Parameters for PCR-amplification of SAMv2 library in preparation for NGS

Cycle number	Denature	Anneal	Extend
1	98 °C, 3 min		
2–23	98 °C, 10 s	63 °C, 10 s	72 °C, 25 s
24			72 °C, 2 min

After PCR-amplification of the library harvested from experimental and control mice using different reverse primers, the pooled library sample is to be submitted for NGS. The recommended read length for the SAMv2 library is 80 bp or above (Joung et al., 2017). The Illumina HiSeq 2500 sequencing platform, which is available at the McMaster Farncombe Institute, can go up to a read length of 250 bp. The highest read length and number of reads available should be used to minimize sequencing error. The NextSeq and MiSeq instruments are also able to satisfy the recommended read length and can be used if the HiSeq2500 is unavailable. The HiSeq2500 also has a minimum of 3×10^8 reads per run which satisfies the $>7 \times 10^6$ reads recommended for the SAMv2 library (>100 reads per sgRNA) (Joung et al., 2017). Paired-end sequencing is unnecessary but will improve the number of reads and therefore decrease sequencing error.

3.8 Bioinformatics: analysis of NGS results to obtain candidate genes

After sequencing, the NGS results for the library distribution can be read using Python. The instructions for this analysis are provided in Joung et al., 2017, with the Python script in Supplementary Data 3 of the publication. The "python count spacers.py" script will output a .csv file containing read counts for each spacer sequence. The output of the Python script will also include a "statistics.txt" file with additional information about the library distribution, including the percentage of sequenced amplicons that are perfect matches (100% overlapping with an actual spacer sequence in the library) and completely depleted spacer sequences. For analyses, only the spacers that are perfect matches should be used (Konermann et al., 2015). As a method of quality control for the sequencing process, the analysis should be continued only if the library shows >70% perfectly matching guides and <0.5% undetected guides (Chen et al., 2015; Joung et al., 2017). Sequencing data that fail to satisfy these conditions should be deemed as poor quality, rendering *in silico* analysis unreliable. Also, any guide with only a single read should be filtered out (Chen et al., 2015). Next, determine the sgRNA fold change that resulted from the screening selection. To do this, add 1 to the read count for each spacer sequence, normalize it to the total number of read counts for that condition (read counts from all spacer sequences), divide the experimental normalized spacer count by the control, and take the base 2 logarithm (Joung et al., 2017).

The next step should be statistical analysis of the fold change for each sgRNA using RIGER. Note that step-by-step instructions for the RIGER analysis are provided in Joung et al., 2017. Analysis using RIGER can be accessed through GENE-E from the Broad Institute (http://www.broadinstitute.org/cancer/software/GENE-E/download.html). To prepare the RIGER input file, create a .csv file with the following column headers (left to right): "WELL_ID," "GENE_ID," and "biorep 1," biorep 2," etc. The WELL_ID column is the list of sgRNA identification numbers, GENE_ID is the list of genes that each sgRNA targets, and the biorep columns show the sgRNA fold change. Start GENE-E and import this .csv file (File > Import > Ranked Lists). Launch RIGER by clicking on Tools, then RIGER. Adjust the settings as per the following recommended values (Joung et al., 2017):

Number of permutations: 1,000,000

Method to convert hairpins to genes: Kolmogorov-Smirnov
Gene rank order: positive to negative for positive selection screens
Select “adjust gene scores”
Select “hairpins are pre-scored”
Hairpin ID: “WELL_ID”
Convert hairpins to: “GENE_ID”

The RIGER analysis will rank genes according to their enrichment in the experimental condition relative to the control condition. The top candidate genes can be determined by using the average ranking of each gene across all the biological replicates of the screen (Joung et al., 2017).

4.0 Discussion and Conclusion

4.1 General discussion points

Some studies of AML relapse suggest that a rare fraction of cells resistant to chemotherapy is responsible for relapse and poor prognosis. These studies involved investigating subclones of AML cells before and after treatment. The findings suggest that certain subclones of mutated HSCs persist through AraC-treatment and likely act as the origin of AML relapse (Shlush et al., 2014, 2017). For example, the DNA methyl transferase 3A (*DNMT3A*)-mutated HSC subclone was found in both diagnosis and remission samples and had a repopulation advantage over healthy HSCs in xenografts. This HSC subclone was thus suggested as being able to survive through chemotherapy and serve as a pool from which relapse could originate (Shlush et al., 2014). Because of such promising discoveries linking AML relapse to stem cells, the conventional model of AML relapse had been that leukemic HSCs persist through anti-neoplastic chemotherapy due to their quiescent state and serve as the origin of relapse (termed the leukemia stem cell (LSC) model). This proposition seemed plausible because, not only are HSCs pluripotent, they also have self-renewal capability to perpetuate themselves. However, two recent studies in AML chemotherapy resistance and relapse have disproven the theory that primitive cells are spared by AraC treatment (Boyd et al., 2018; Farge et al., 2017). Not only did these studies find that the primitive subpopulation ($CD34^+$, $CD38^-$) gets recruited into the cell cycle and depleted during AraC treatment, they found that certain transcriptional signatures correlated with relapse were consistently found after *in vivo* AraC treatment (Boyd et al., 2018; Farge et al., 2017). One of these studies reported increased transcription of genes related to oxidative phosphorylation and fatty acid oxidation in chemo-resistant AML cells (ex. ABCB10, CD36 gene), suggesting an elevated rate of respiration correlated with chemo-resistance (Farge et al., 2017). The other study reported increased transcription of genes involved in a wide variety of functions that relied on G-protein-coupled receptor (GPCR) signalling (Boyd et al., 2018). In this second study, the cells exhibiting this transcriptional signature were termed leukemia regenerating cells (LRCs). Interestingly, this transcriptional signature was induced by AraC treatment itself, suggesting that AraC may, ironically, be conducive to the relapse phenomenon (Boyd et al., 2018).

The LRCs were reported to arise beginning at the post-chemotherapy residual disease state, and only in patient-derived xenografts of AML as opposed to those of healthy HSCs (Boyd et al., 2018). Interestingly, the LRC state was found to arise only shortly after *in vivo* AraC treatment, while being absent from AML cells treated *in vitro* (Boyd et al., 2018). Furthermore, the LRC state was observed when the AML cells *in vitro* were exposed to the serum of AraC-treated mice, suggesting that the relapse phenomenon is dependent on cell extrinsic factors in order to occur (Boyd et al., 2018). The idea that cancer is dependent on cell extrinsic factors was not new. In a study that carried out an shRNA genetic screening for genes responsible for the survival and maintenance of glioblastoma cells, the overlap in hits between the *in vitro* and *in vivo* screens were limited to only housekeeping genes and positive controls (Miller et al., 2017). Just as the intracranial environment exerts different physical conditions for glioblastoma, it seems that the same concept is applicable to AML wherein the bone marrow microenvironment or blood serum are a critical influence on the phenotypes that are enriched in relapse. This similarity between the two cancers can be observed despite the

fact one is a solid tumor while the other is a liquid tumor. The importance of the microenvironment in AML relapse justifies the choice to have designed the CRISPRa screen to take place *in vivo* as opposed to *in vitro*. Even if several candidate genes are found in an *in vitro* genome-wide screen, they would have negligible merit in further validation studies due to their irrelevance to the clinical manifestation of AML.

Besides the genes associated with oxidative phosphorylation and fatty acid oxidation mentioned previously, there are many genes that have been implicated in chemotherapy-resistance and relapse of AML. Notably, the dopamine receptor D2 (*DRD2*) was found to be one of the LRC markers, and was also shown to be targetable to decrease blast counts in refractory/relapsed AML patients during clinical trial of the drug, thioridazine (Aslostovar et al., 2018; Boyd et al., 2018). Not only did thioridazine reduce blast counts, the upregulation of *DRD2* during the LRC state was found to be mitigated *in vivo* (Boyd et al., 2018). The *DRD2* gene is not only implicated in AML relapse, as it is found to be upregulated in many other cancers including cervical (Mao et al., 2015), lung (Kanakis et al., 2015), esophageal (L. Li et al., 2006), breast (Pornour et al., 2015), ovarian (Moreno-Smith et al., 2011), neuroblastoma (Deslauriers et al., 2011), and glioma (J. Li et al., 2014). In addition to *DRD2*, the 5-hydroxytryptamine receptor 4 (HTR4), which is a serotonin receptor, was also found to be one of the LRC markers (Boyd et al., 2018). The recurring implication of *DRD2* in AML and many other cancers, combined with *HTR4* as an LRC marker suggests that neurotransmitter receptors, including *DRD2* and *HTR4*, are highly likely to present as candidate genes in the CRISPRa screen.

Despite the clear strengths of the designed CRISPRa screen described in this thesis, its inherent weaknesses must also be acknowledged. Perhaps the most obvious weakness is that it uses a cell line, which has minimal clinical relevance. In reality, AML is a vastly heterogenous disease that presents multiple subclones, and the blood is composed of cells at various hematopoietic differentiation stages. While the decision to use a cell line in this screen is still valid because the homogeneity offered by a cell line eliminates the possibility that the hits may be linked to the subclone/cell type in which they were found, this approach is limited in clinical relevance. To consolidate this weakness, single-cell RNA sequencing (scRNA-seq) should be done using paired primary AML samples, obtained from the same patient both before and after chemotherapy, to determine the genes that are relatively upregulated after chemotherapy. Because scRNA-seq enables analysis of transcriptional signatures in each individual cell, the issue of heterogeneity can be resolved. If the candidate genes identified from the CRISPRa screen overlap with the upregulated genes identified in the scRNA-seq experiment, there would be greater confidence that these shortlisted candidate genes are true "hits." By this approach, the CRISPRa screen is able to address causality (between genes and relapse), while the scRNA-seq is able to address AML heterogeneity and clinical relevance.

There are many experiments that should be done to further validate the candidate genes identified from the CRISPRa screen and scRNA-seq. First, genetic intervention of these genes should be tested to determine if they have any influence on the frequency or aggressiveness of the post-chemotherapy relapse. Overexpression vectors targeting each of these genes should be tested individually in xenografts to confirm whether they have a proliferative advantage during relapse over xenografts of the empty-vector control. In parallel, knockouts or repression of these genes should also be tested to determine if relapse is prevented or mitigated. Similar to knockdown or repression of candidate genes, *in vivo* drug intervention of these genes can also be tested for the same goal. Finding drugs for the prevention of relapse would have a much higher clinical translation potential than genetic intervention methods because drugs are easier to test and

administer in patients. In the ideal case, drugs that present positive results in the prevention of relapse could be administered to patients in conjunction with conventional chemotherapy (7+3 regimen) to pre-emptively avert relapse while reducing leukemic burden at the same time.

Another technical challenge of the CRISPRa screen is that, because only a single sgRNA enters each cell, it is difficult to determine from the screen alone whether AML relapse is driven by synergistic effects of multiple genes. To resolve this issue, the top few overlapping candidate genes from the CRISPRa screen and scRNA-seq can be used to run multiple, smaller screens using various combinations of sgRNAs. If xenografts of these multi-sgRNA cells survive at a higher rate than those that are delivered only 1 of the sgRNAs, it would suggest synergy between the corresponding genes. In this case, the most practical approach would be to deliver 2 sgRNAs into each cell using a total of 3 vectors: MPH + 2 vectors carrying sgRNA. To alleviate the 3 potentially excessive antibiotic selections required for the transductions, a fluorescent marker may need to be incorporated into one of the vectors for purification via fluorescence activated cell sorting (FACS). Unlike the suggested experiments mentioned previously, this experiment serves a supplementary purpose rather than the validation of candidate genes.

In the PCR-amplification of the library before NGS, there are 8 unique barcodes available in the reverse primers. These barcodes can be used to pool different samples together for a single sequencing run. For example, the library harvested from the untreated control group can be amplified using NGS-Lib-SAM-Rev-1, while the AraC-treated experimental group can be amplified using NGS-Lib-SAM-Rev-2. This way, the library from both groups can be pooled for a single sequencing. Alternatively, a different reverse primer can be used to amplify the library from each individual mouse in the experimental group. This way, the level of enrichment of candidate genes can be analyzed in each mouse, improving the confidence that these genes are true hits if they are found enriched in every experimental group mouse. However, because each mouse alone does not satisfy the 100x coverage at the time of AraC treatment, the library distribution arising from each mouse cannot be deemed a confident representation of the change in library distribution (discussed further in next subsection). Also, there is not enough reverse primers to account for all individual mice, so a few mice will have to use the same reverse primer.

The bioinformatic analysis of the NGS results by RIGER computes gene rankings according to the genes' enrichment in the experimental group relative to the control group. In other words, it assumes that the candidate genes are the ones that are enriched in the AraC-treated experimental group while being low or absent from the untreated control group. This implies that genes enriched in both the experimental and control groups are disregarded with the assumption that they represent genes that generally promote survival, engraftment, and/or proliferation *in vivo*, with no association with AML relapse causation. This approach, however, is vulnerable to the loss of potential true hits. Genes that promote engraftment and proliferation of AML cells in the bone marrow, for example, can potentially be causative for relapse while also being present in the untreated control group. This weakness does not stem from RIGER and would be present regardless of which statistical analysis tool is used. It can be mitigated, however, by taking the overlaps in candidate genes between the CRISPRa screen and the scRNA-seq described above. Any genes that are highly enriched in both the experimental and control groups can be cross checked with the results of the scRNA-seq data to determine if they are upregulated post-chemotherapy. Because the scRNA-seq uses primary samples and not PDX, the genes that are enriched in both the experimental and control groups of the CRISPRa screen can be suspected as being relapse-causative and not engraftment-promoting. Note that this cross check with the scRNA-seq data must be done before RIGER analysis, using the library distribution output from

Python. This is because RIGER computes the enrichment of genes in the experimental group relative to the control group, while the Python output file shows the library distribution in the two groups separately without comparison.

The method of normalizing the frequency of each sgRNA after sequencing as described in the Methods section involve linear normalization. This means that an sgRNA read 10 times in a total of 1000 reads is assumed to have the same read count as an sgRNA read 100 times in a total of 10,000 reads. This ensures that variance in total read counts is accounted for before outputting the ranked order of sgRNAs in each condition and replicate. This approach is simple and straightforward but may fail to address technical variation. Technical variation refers to variation caused by conditions in the experimental procedures that are difficult to control (Scherer, 2009). Technical variation often leads to variation in global properties, which includes the total number of unique sgRNAs detected and the median read count of each sgRNA (Hicks & Irizarry, 2014). To control for technical variation, quantile normalization is sometimes used in genetic expression studies and genome screens (Bachas et al., 2018; B. Li et al., 2020; Parnas et al., 2015). Originally developed for gene expression microarrays, this is a non-linear transformation method that, in the context of this CRISPRa screen, would replace the read count of each sgRNA from each mouse with the mean read count across all mice in that condition with the same rank, or "quantile" (Hicks & Irizarry, 2014). Thus, this method requires different barcodes to be used during PCR-amplification of spacers from each mouse of each condition. The most significant risk of using this approach is that it assumes that the statistical distribution of the sgRNAs is the same across all mice for each condition. Thus, to use quantile normalization, the minimum coverage required to consistently output the same library distribution in each mouse of each condition would have be known. The method of determining this minimum coverage is discussed in the next subsection.

4.2 Mitigating the limitations of cell line surrogacy

The methods of the CRISPRa screen described in this thesis are based on a cell line derived xenograft serving as a surrogate to the actual, clinical manifestation of AML. There are several points to consider in this approach. Notably, it must be acknowledged that cell lines are genetically unstable over time and may develop new subclones with increasing passage numbers, leading to heterogenous populations (Ng et al., 2017). This means that the OCI-AML3 cell line must be used at low passage numbers to maintain the advantage of homogeneity mentioned previously. However, while it is preferable to run the screen with a homogenous population, it may not be a critical factor in determining relapse-causative genes because the LRC and LSC models do not depend on AML patient genetics – studies characterizing the two models did not sample from patients of particular genetic subgroups (Boyd et al., 2018; Ng et al., 2016). Therefore, heterogeneity and homogeneity of the cells used for the screen are important to consider, but not critical. Furthermore, if the CRISPRa screen shows hits overlapping with the scRNA-seq results and LRC signature while using a cell line, it would consolidate the argument that the clonal heterogeneity of AML has minimal relation to relapse and that the use of a cell line was enough to capture the causative genes. While one could argue that the OCI-AML3 cell line chosen could be inherently incapable of producing the LRC signature in response to AraC treatment due to a rare genetic variation, with enough resources and time multiple AML cell lines could be transplanted simultaneously to determine which cell lines produce the LRC signature upon AraC treatment.

It was previously stated that different barcodes on each reverse primer could be utilized to pool the harvested library from multiple mice and determine whether the same candidate genes could be identified across all mice. The biggest argument against this approach would be that it is unclear whether the coverage provided by each individual mouse is sufficient to accurately output the same library distributions and candidate genes. To address this issue, a limiting dilution assay can be done using decreasing numbers of transplanted OCI-AML3 cells. If the same candidate genes are consistently found in high frequencies down to a certain transplant cell dose, it would indicate that the coverage provided by this cell dose is the minimum at which candidate genes can be reliably determined. Validation experiments following the screen should then focus on candidate genes arising from multiple mice, at or above this minimum coverage, as these offer higher confidence as being relapse-causative. Furthermore, the minimum reliable coverage determined in this limiting dilution assay could also be used to allow quantile normalization, as described in the previous subsection, to mitigate the effects of technical variation. A proposed workflow of the screen incorporating the limiting dilution assay is shown in Figure 4.1.

A potential weakness in the CRISPRa screen as designed in this thesis is that it attempts to capture the relapse-causative genes at a single timepoint several weeks following chemotherapy. This is significant because one of the goals of this study is to find potential overlaps with the LRC transcriptional signature, which is transiently expressed shortly after chemotherapy (Boyd et al., 2018). If the costs of additional mice can be afforded, the CRISPRa screen should ideally include harvest points along the recovery kinetics following chemotherapy. The multiple harvest points in the CRISPRa screen should also be accompanied by multiple points in the scRNA-seq as well during the post-chemotherapy kinetics to allow for overlap comparison between the CRISPRa screen and scRNA-seq data.

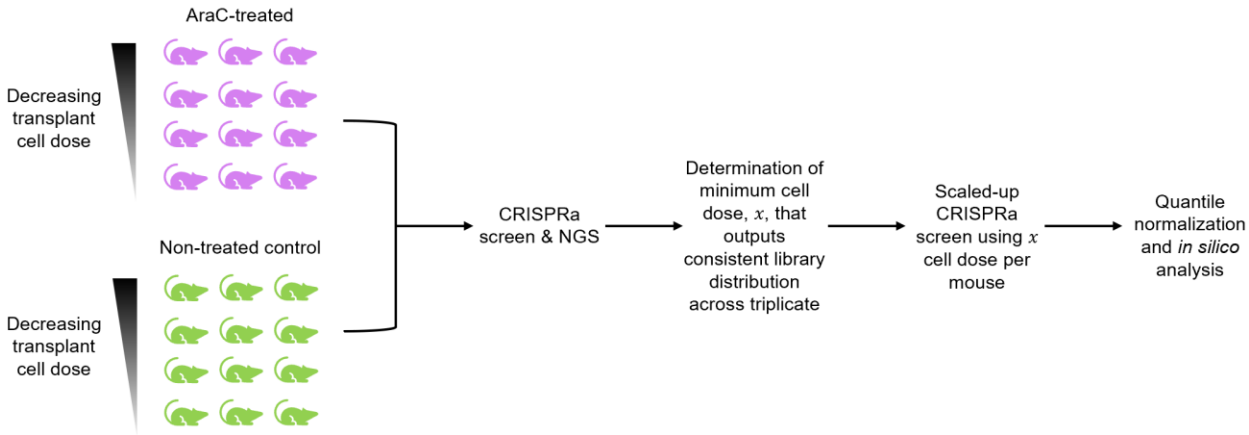

Figure 4.1: Proposed CRISPRa screen with incorporated limiting dilution assay to allow quantile normalization.

Cells are transplanted at decreasing cell doses, followed by the CRISPRa screen and Next Gen Sequencing. The cell dose that outputs consistent library distribution across the triplicate is determined. The CRISPRa screen is repeated using the determined cell dose at a higher scale to allow higher coverage and increased confidence. Different reverse primers used for PCR-amplification of the library harvested from each mouse allow quantile normalization, which controls for technical variation.

4.3 Conclusion

The optimized procedures for the genome-wide screening described in this thesis aim to better understand the genetic cause for post-chemotherapy relapse of AML. Once candidate genes are validated by subsequent experiments as causal and candidate drugs for relapse intervention are found, the results of this project could potentially adapt the current 7+3 regimen to address the issue of relapse before it occurs.

5.0 Bibliography

Almeida, A. M., & Ramos, F. (2016). Acute myeloid leukemia in the older adults. *Leukemia Research Reports*, *6*, 1–7. https://doi.org/10.1016/j.lrr.2016.06.001

Almosailleakh, M., & Schwaller, J. (2019). Murine models of acute Myeloid Leukaemia. In *International Journal of Molecular Sciences*. https://doi.org/10.3390/ijms20020453

Anders, C., Niewoehner, O., Duerst, A., & Jinek, M. (2014). Structural basis of PAM-dependent target DNA recognition by the Cas9 endonuclease. *Nature*. https://doi.org/10.1038/nature13579

Andresen, V., Erikstein, B. S., Mukherjee, H., Sulen, A., Popa, M., Sørnes, S., Reikvam, H., Chan, K.-P., Hovland, R., McCormack, E., Bruserud, Ø., Myers, A. G., & Gjertsen, B. T. (2016). Anti-proliferative activity of the NPM1 interacting natural product avrainvillamide in acute myeloid leukemia. *Cell Death & Disease*, *7*(12), e2497. https://doi.org/10.1038/cddis.2016.392

Aslostovar, L., Boyd, A. L., Almakadi, M., Collins, T. J., Leong, D. P., Tirona, R. G., Kim, R. B., Julian, J. A., Xenocostas, A., Leber, B., Levine, M. N., Foley, R., & Bhatia, M. (2018). A phase 1 trial evaluating thioridazine in combination with cytarabine in patients with acute myeloid leukemia. *Blood Advances*, *2*(15), 1935–1945. https://doi.org/10.1182/bloodadvances.2018015677

Bachas, C., Hodzic, J., van der Mijn, J. C., Stoepker, C., Verheul, H. M. W., Wolthuis, R. M. F., Felley-Bosco, E., van Wieringen, W. N., van Beusechem, V. W., Brakenhoff, R. H., & de Menezes, R. X. (2018). Rscreenorm: Normalization of CRISPR and siRNA screen data for more reproducible hit selection. *BMC Bioinformatics*. https://doi.org/10.1186/s12859-018-2306-z

Balusu, R., Fiskus, W., Rao, R., Chong, D. G., Nalluri, S., Mudunuru, U., Ma, H., Chen, L., Venkannagari, S., Ha, K., Abhyankar, S., Williams, C., McGuirk, J., Khoury, H. J., Ustun, C., & Bhalla, K. N. (2011). Targeting levels or oligomerization of nucleophosmin 1 induces differentiation and loss of survival of human AML cells with mutant NPM1. *Blood*, *118*(11), 3096–3106. https://doi.org/10.1182/blood-2010-09-309674

Berns, K., Hijmans, E. M., Mullenders, J., Brummelkamp, T. R., Velds, A., Heimerikx, M., Kerkhoven, R. M., Madlredjo, M., Nijkamp, W., Weigelt, B., Agami, R., Ge, W., Cavet, G., Linsley, P. S., Beijersbergen, R. L., & Bernards, R. (2004). A large-scale RNAi screen in human cells identifies new components of the p53 pathway. *Nature*. https://doi.org/10.1038/nature02371

Bierhuizen, M. F., Westerman, Y., Hartong, S. C., Visser, T. P., Wognum, A. W., & Wagemaker, G. (1999). Efficient detection and selection of immature rhesus monkey and human CD34+ hematopoietic cells expressing the enhanced green fluorescent protein (EGFP). *Leukemia*. https://doi.org/10.1038/sj.leu.2401374

Boettcher, M., & McManus, M. T. (2015). Choosing the Right Tool for the Job: RNAi, TALEN, or CRISPR. In *Molecular Cell*. https://doi.org/10.1016/j.molcel.2015.04.028

Bonnet, D., & Dick, J. E. (1997). Human acute myeloid leukemia is organized as a hierarchy that originates from a primitive hematopoietic cell. *Nature Medicine*. https://doi.org/10.1038/nm0797-730

Borthakur, G., Duvvuri, S., Ruvolo, V., Tripathi, D. N., Piya, S., Burks, J., Jacamo, R., Kojima, K., Ruvolo, P., Fueyo-Margareto, J., Konopleva, M., & Andreeff, M. (2015). MDM2 Inhibitor, Nutlin 3a, Induces p53 Dependent Autophagy in Acute Leukemia by AMP Kinase

Activation. *PloS One*, *10*(10), e0139254. https://doi.org/10.1371/journal.pone.0139254
Bose, P., Vachhani, P., & Cortes, J. E. (2017). Treatment of Relapsed/Refractory Acute Myeloid Leukemia. *Current Treatment Options in Oncology*, *18*(3), 17. https://doi.org/10.1007/s11864-017-0456-2
Boutros, M., Kiger, A. A., Armknecht, S., Kerr, K., Hild, M., Koch, B., Haas, S. A., Paro, R., & Perrimon, N. (2004). Genome-Wide RNAi Analysis of Growth and Viability in Drosophila Cells. *Science*. https://doi.org/10.1126/science.1091266
Box, J. K., Paquet, N., Adams, M. N., Boucher, D., Bolderson, E., O'Byrne, K. J., & Richard, D. J. (2016). Nucleophosmin: from structure and function to disease development. *BMC Molecular Biology*, *17*(1), 19. https://doi.org/10.1186/s12867-016-0073-9
Boyd, A. L., Aslostovar, L., Reid, J., Ye, W., Tanasijevic, B., Porras, D. P., Shapovalova, Z., Almakadi, M., Foley, R., Leber, B., Xenocostas, A., & Bhatia, M. (2018). Identification of Chemotherapy-Induced Leukemic-Regenerating Cells Reveals a Transient Vulnerability of Human AML Recurrence. *Cancer Cell*, *34*(3), 483-498.e5. https://doi.org/10.1016/J.CCELL.2018.08.007
Bryder, D., Rossi, D. J., & Weissman, I. L. (2006). Hematopoietic stem cells: The paradigmatic tissue-specific stem cell. *American Journal of Pathology*. https://doi.org/10.2353/ajpath.2006.060312
Burger, O., Ashtamker, G. F., Bercovich, N., Rusanovsky, M., Pinzur, L., Jacov, O. M., Carmi, N. D., Meiron, M., Lior, L., Meretzki, S., Prather, W. R., Kadouri, A., Treves, A. J., Rowe, J. M., Horwitz, E. M., & Nagler, A. (2007). Human Placental Derived Mesenchymal Stromal Cells (MSC) Grown in 3D-Culture (PLX-I), Promotes Engraftment of Human Umbilical Cord Blood (hUCB) Derived CD34+ Cells in NOD/SCID Mice. *Blood*. https://doi.org/10.1182/blood.v110.11.1416.1416
Caldarelli, A., Müller, J. P., Paskowski-Rogacz, M., Herrmann, K., Bauer, R., Koch, S., Heninger, A. K., Krastev, D., Ding, L., Kasper, S., Fischer, T., Brodhun, M., Böhmer, F.-D., & Buchholz, F. (2013). A genome-wide RNAi screen identifies proteins modulating aberrant FLT3-ITD signaling. *Leukemia*, *27*(12), 2301–2310. https://doi.org/10.1038/leu.2013.83
Cao, X., Shores, E. W., Hu-Li, J., Anver, M. R., Kelsail, B. L., Russell, S. M., Drago, J., Noguchi, M., Grinberg, A., Bloom, E. T., Paul, W. E., Katz, S. I., Love, P. E., & Leonard, W. J. (1995). Defective lymphoid development in mice lacking expression of the common cytokine receptor γ chain. *Immunity*. https://doi.org/10.1016/1074-7613(95)90047-0
Caocci, G., Greco, M., & La Nasa, G. (2017). Bone Marrow Homing and Engraftment Defects of Human Hematopoietic Stem and Progenitor Cells. *Mediterranean Journal of Hematology and Infectious Diseases*, *9*(1), e2017032. https://doi.org/10.4084/MJHID.2017.032
CHANG, H.-Y., RODRIGUEZ, V., NARBONI, G., BODEY, G. P., LUNA, M. A., & FREIREICH, E. J. (1976). CAUSES OF DEATH IN ADULTS WITH ACUTE LEUKEMIA. *Medicine*, *55*(3), 259–268. https://doi.org/10.1097/00005792-197605000-00005
Chen, S., Sanjana, N. E., Zheng, K., Shalem, O., Lee, K., Shi, X., Scott, D. A., Song, J., Pan, J. Q., Weissleder, R., Lee, H., Zhang, F., & Sharp, P. A. (2015). Genome-wide CRISPR screen in a mouse model of tumor growth and metastasis. *Cell*. https://doi.org/10.1016/j.cell.2015.02.038
Chen, Y.-L., Chueh, F.-S., Yang, J.-S., Hsueh, S.-C., Lu, C.-C., Chiang, J.-H., Lee, C.-S., Lu, H.-F., & Chung, J.-G. (2015). Antitumor effects with apoptotic death in human promyelocytic

leukemia HL-60 cells and suppression of leukemia xenograft tumor growth by irinotecan HCl. *Environmental Toxicology*, *30*(7), 803–815. https://doi.org/10.1002/tox.21959

Cho, B.-S., Zeng, Z., Mu, H., Wang, Z., Konoplev, S., McQueen, T., Protopopova, M., Cortes, J., Marszalek, J. R., Peng, S.-B., Ma, W., Davis, R. E., Thornton, D. E., Andreeff, M., & Konopleva, M. (2015). Antileukemia activity of the novel peptidic CXCR4 antagonist LY2510924 as monotherapy and in combination with chemotherapy. *Blood*, *126*(2), 222–232. https://doi.org/10.1182/blood-2015-02-628677

Cline, S. D., & Osheroff, N. (1999). Cytosine arabinoside lesions are position-specific topoisomerase II poisons and stimulate DNA cleavage mediated by the human type II enzymes. *The Journal of Biological Chemistry*, *274*(42), 29740–29743. https://doi.org/10.1074/jbc.274.42.29740

Cohen, S. S. (1977). The mechanisms of lethal action of arabinosyl cytosine (araC) and arabinosyl adenine (araA). *Cancer*, *40*(1 Suppl), 509–518. http://www.ncbi.nlm.nih.gov/pubmed/328134

Colvin, G. A., Lambert, J. F., Abedi, M., Hsieh, C. C., Carlson, J. E., Stewart, F. M., & Quesenberry, P. J. (2004). Murine marrow cellularity and the concept of stem cell competition: Geographic and quantitative determinants in stem cell biology. *Leukemia*. https://doi.org/10.1038/sj.leu.2403268

Corces, M. R., Buenrostro, J. D., Wu, B., Greenside, P. G., Chan, S. M., Koenig, J. L., Snyder, M. P., Pritchard, J. K., Kundaje, A., Greenleaf, W. J., Majeti, R., & Chang, H. Y. (2016). Lineage-specific and single-cell chromatin accessibility charts human hematopoiesis and leukemia evolution. *Nature Genetics*, *48*(10), 1193–1203. https://doi.org/10.1038/ng.3646

Damaraju, V. L., Damaraju, S., Young, J. D., Baldwin, S. A., Mackey, J., Sawyer, M. B., & Cass, C. E. (2003). Nucleoside anticancer drugs: The role of nucleoside transporters in resistance to cancer chemotherapy. In *Oncogene*. https://doi.org/10.1038/sj.onc.1206952

De Greef, G. E., Van Putten, W. L. J., Boogaerts, M., Huijgens, P. C., Verdonck, L. F., Vellenga, E., Theobald, M., Jacky, E., & Löwenberg, B. (2005). Criteria for defining a complete remission in acute myeloid leukaemia revisited. An analysis of patients treated in HOVON-SAKK co-operative group studies. *British Journal of Haematology*. https://doi.org/10.1111/j.1365-2141.2004.05285.x

De Kouchkovsky, I., & Abdul-Hay, M. (2016). 'Acute myeloid leukemia: a comprehensive review and 2016 update.' *Blood Cancer Journal*, *6*(7), e441–e441. https://doi.org/10.1038/bcj.2016.50

Deslauriers, J., Lefrançois, M., Larouche, A., Sarret, P., & Grignon, S. (2011). Antipsychotic-induced DRD2 upregulation and its prevention by α-lipoic acid in SH-SY5Y neuroblastoma cells. *Synapse (New York, N.Y.)*, *65*(4), 321–331. https://doi.org/10.1002/syn.20851

Döhner, H., Estey, E., Grimwade, D., Amadori, S., Appelbaum, F. R., Büchner, T., Dombret, H., Ebert, B. L., Fenaux, P., Larson, R. A., Levine, R. L., Lo-Coco, F., Naoe, T., Niederwieser, D., Ossenkoppele, G. J., Sanz, M., Sierra, J., Tallman, M. S., Tien, H. F., … Bloomfield, C. D. (2017). Diagnosis and management of AML in adults: 2017 ELN recommendations from an international expert panel. In *Blood* (Vol. 129, Issue 4, pp. 424–447). American Society of Hematology. https://doi.org/10.1182/blood-2016-08-733196

Döhner, H., Weisdorf, D. J., & Bloomfield, C. D. (2015). Acute Myeloid Leukemia. *New England Journal of Medicine*, *373*(12), 1136–1152. https://doi.org/10.1056/NEJMra1406184

Duran-Struuck, R., & Dysko, R. C. (2009). Principles of bone marrow transplantation (BMT):

Providing optimal veterinary and husbandry care to irradiated mice in BMT studies. In *Journal of the American Association for Laboratory Animal Science*.

Farge, T., Saland, E., de Toni, F., Aroua, N., Hosseini, M., Perry, R., Bosc, C., Sugita, M., Stuani, L., Fraisse, M., Scotland, S., Larrue, C., Boutzen, H., Féliu, V., Nicolau-Travers, M.-L., Cassant-Sourdy, S., Broin, N., David, M., Serhan, N., … Sarry, J.-E. (2017a). Chemotherapy-Resistant Human Acute Myeloid Leukemia Cells Are Not Enriched for Leukemic Stem Cells but Require Oxidative Metabolism. *Cancer Discovery*, *7*(7), 716–735. https://doi.org/10.1158/2159-8290.CD-16-0441

Farge, T., Saland, E., de Toni, F., Aroua, N., Hosseini, M., Perry, R., Bosc, C., Sugita, M., Stuani, L., Fraisse, M., Scotland, S., Larrue, C., Boutzen, H., Féliu, V., Nicolau-Travers, M.-L., Cassant-Sourdy, S., Broin, N., David, M., Serhan, N., … Sarry, J.-E. (2017b). Chemotherapy-Resistant Human Acute Myeloid Leukemia Cells Are Not Enriched for Leukemic Stem Cells but Require Oxidative Metabolism. *Cancer Discovery*, *7*(7), 716–735. https://doi.org/10.1158/2159-8290.CD-16-0441

Floc'h, N., Ashton, S., Taylor, P., Trueman, D., Harris, E., Odedra, R., Maratea, K., Derbyshire, N., Caddy, J., Jacobs, V. N., Hattersley, M., Wen, S., Curtis, N. J., Pilling, J. E., Pease, E. J., & Barry, S. T. (2017). *Optimizing Therapeutic Effect of Aurora B Inhibition in Acute Myeloid Leukemia with AZD2811 Nanoparticles*. https://doi.org/10.1158/1535-7163.MCT-16-0580

Garneau, J. E., Dupuis, M. È., Villion, M., Romero, D. A., Barrangou, R., Boyaval, P., Fremaux, C., Horvath, P., Magadán, A. H., & Moineau, S. (2010). The CRISPR/cas bacterial immune system cleaves bacteriophage and plasmid DNA. *Nature*. https://doi.org/10.1038/nature09523

Green, A. S., Maciel, T. T., Hospital, M.-A., Yin, C., Mazed, F., Townsend, E. C., Pilorge, S., Lambert, M., Paubelle, E., Jacquel, A., Zylbersztejn, F., Decroocq, J., Poulain, L., Sujobert, P., Jacque, N., Adam, K., So, J. C. C., Kosmider, O., Auberger, P., … Tamburini, J. (2015). Pim kinases modulate resistance to FLT3 tyrosine kinase inhibitors in FLT3-ITD acute myeloid leukemia. *Science Advances*, *1*(8), e1500221. https://doi.org/10.1126/sciadv.1500221

He, L., Shi, L., Du, Z., Huang, H., Gong, R., Ma, L., Chen, L., Gao, S., Lyu, J., & Gu, H. (2018). Mebendazole exhibits potent anti-leukemia activity on acute myeloid leukemia. *Experimental Cell Research*, *369*(1), 61–68. https://doi.org/10.1016/J.YEXCR.2018.05.006

Heydt, Q., Larrue, C., Saland, E., Bertoli, S., Sarry, J.-E., Besson, A., Manenti, S., Joffre, C., & Mansat-De Mas, V. (2018). Oncogenic FLT3-ITD supports autophagy via ATF4 in acute myeloid leukemia. *Oncogene*, *37*(6), 787–797. https://doi.org/10.1038/onc.2017.376

Hicks, S. C., & Irizarry, R. A. (2014). When to use Quantile Normalization? *BioRxiv*. https://doi.org/10.1101/012203

Ishino, Y., Shinagawa, H., Makino, K., Amemura, M., & Nakata, A. (1987). Nucleotide sequence of the iap gene, responsible for alkaline phosphatase isozyme conversion in Escherichia coli, and identification of the gene product. *Journal of Bacteriology*, *169*(12), 5429–5433. https://doi.org/10.1128/jb.169.12.5429-5433.1987

Ito, M., Hiramatsu, H., Kobayashi, K., Suzue, K., Kawahata, M., Hioki, K., Ueyama, Y., Koyanagi, Y., Sugamura, K., Tsuji, K., Heike, T., & Nakahata, T. (2002). NOD/SCID/γcnull mouse: An excellent recipient mouse model for engraftment of human cells. *Blood*. https://doi.org/10.1182/blood-2001-12-0207

Jagannathan-Bogdan, M., & Zon, L. I. (2013). Hematopoiesis. *Development (Cambridge,*

England), *140*(12), 2463–2467. https://doi.org/10.1242/dev.083147

Jansen, R., Van Embden, J. D. A., Gaastra, W., & Schouls, L. M. (2002). Identification of genes that are associated with DNA repeats in prokaryotes. *Molecular Microbiology*, *43*(6), 1565–1575. https://doi.org/10.1046/j.1365-2958.2002.02839.x

Jian, P., Li, Z. W., Fang, T. Y., Jian, W., Zhuan, Z., Mei, L. X., Yan, W. S., & Jian, N. (2011). Retinoic acid induces HL-60 cell differentiation via the upregulation of miR-663. *Journal of Hematology & Oncology*, *4*, 20. https://doi.org/10.1186/1756-8722-4-20

Jinek, M., Chylinski, K., Fonfara, I., Hauer, M., Doudna, J. A., & Charpentier, E. (2012). A programmable dual-RNA-guided DNA endonuclease in adaptive bacterial immunity. *Science*. https://doi.org/10.1126/science.1225829

Joung, J., Konermann, S., Gootenberg, J. S., Abudayyeh, O. O., Platt, R. J., Brigham, M. D., Sanjana, N. E., & Zhang, F. (2017). Genome-scale CRISPR-Cas9 knockout and transcriptional activation screening. *Nature Protocols*, *12*(4), 828–863. https://doi.org/10.1038/nprot.2017.016

Kanakis, G., Grimelius, L., Spathis, A., Tringidou, R., Rassidakis, G. Z., Öberg, K., Kaltsas, G., & Tsolakis, A. V. (2015). Expression of Somatostatin Receptors 1-5 and Dopamine Receptor 2 in Lung Carcinoids: Implications for a Therapeutic Role. *Neuroendocrinology*, *101*(3), 211–222. https://doi.org/10.1159/000381061

Khwaja, A., Bjorkholm, M., Gale, R. E., Levine, R. L., Jordan, C. T., Ehninger, G., Bloomfield, C. D., Estey, E., Burnett, A., Cornelissen, J. J., Scheinberg, D. A., Bouscary, D., & Linch, D. C. (2016). Acute myeloid leukaemia. *Nature Reviews Disease Primers*, *2*, 16010. https://doi.org/10.1038/nrdp.2016.10

Konermann, S., Brigham, M. D., Trevino, A. E., Joung, J., Abudayyeh, O. O., Barcena, C., Hsu, P. D., Habib, N., Gootenberg, J. S., Nishimasu, H., Nureki, O., & Zhang, F. (2015). Genome-scale transcriptional activation by an engineered CRISPR-Cas9 complex. *Nature*, *517*(7536), 583–588. https://doi.org/10.1038/nature14136

König, R., Chiang, C. Y., Tu, B. P., Yan, S. F., DeJesus, P. D., Romero, A., Bergauer, T., Orth, A., Krueger, U., Zhou, Y., & Chanda, S. K. (2007). A probability-based approach for the analysis of large-scale RNAi screens. *Nature Methods*. https://doi.org/10.1038/nmeth1089

Kumar, C. C. (2011). Genetic abnormalities and challenges in the treatment of acute myeloid leukemia. *Genes & Cancer*, *2*(2), 95–107. https://doi.org/10.1177/1947601911408076

L.D., S., M.A., B., J., V. G.-M., & D.L., G. (2012). Humanized mice for immune system investigation: Progress, promise and challenges. In *Nature Reviews Immunology*.

Li, B., Clohisey, S. M., Chia, B. S., Wang, B., Cui, A., Eisenhaure, T., Schweitzer, L. D., Hoover, P., Parkinson, N. J., Nachshon, A., Smith, N., Regan, T., Farr, D., Gutmann, M. U., Bukhari, S. I., Law, A., Sangesland, M., Gat-Viks, I., Digard, P., … Hacohen, N. (2020). Genome-wide CRISPR screen identifies host dependency factors for influenza A virus infection. *Nature Communications*. https://doi.org/10.1038/s41467-019-13965-x

Li, J., Zhu, S., Kozono, D., Ng, K., Futalan, D., Shen, Y., Akers, J. C., Steed, T., Kushwaha, D., Schlabach, M., Carter, B. S., Kwon, C.-H., Furnari, F., Cavenee, W., Elledge, S., & Chen, C. C. (2014). Genome-wide shRNA screen revealed integrated mitogenic signaling between dopamine receptor D2 (DRD2) and epidermal growth factor receptor (EGFR) in glioblastoma. *Oncotarget*, *5*(4), 882–893. https://doi.org/10.18632/oncotarget.1801

Li, L., Miyamoto, M., Ebihara, Y., Mega, S., Takahashi, R., Hase, R., Kaneko, H., Kadoya, M., Itoh, T., Shichinohe, T., Hirano, S., & Kondo, S. (2006). DRD2/DARPP-32 expression correlates with lymph node metastasis and tumor progression in patients with esophageal

squamous cell carcinoma. *World Journal of Surgery*, *30*(9), 1672–1679; discussion 1680-1. https://doi.org/10.1007/s00268-006-0035-3

Li, S., Mason, C. E., & Melnick, A. (2016). Genetic and epigenetic heterogeneity in acute myeloid leukemia. *Current Opinion in Genetics & Development*, *36*, 100–106. https://doi.org/10.1016/j.gde.2016.03.011

Mambet, C., Chivu-Economescu, M., Matei, L., Necula, L. G., Dragu, D. L., Bleotu, C., & Diaconu, C. C. (2018). Murine models based on acute myeloid leukemia-initiating stem cells xenografting. *World Journal of Stem Cells*, *10*(6), 57–65. https://doi.org/10.4252/wjsc.v10.i6.57

Mao, M., Yu, T., Hu, J., & Hu, L. (2015). Dopamine D2 receptor blocker thioridazine induces cell death in human uterine cervical carcinoma cell line SiHa. *Journal of Obstetrics and Gynaecology Research*, *41*(8), 1240–1245. https://doi.org/10.1111/jog.12691

Miller, T. E., Liau, B. B., Wallace, L. C., Morton, A. R., Xie, Q., Dixit, D., Factor, D. C., Kim, L. J. Y., Morrow, J. J., Wu, Q., Mack, S. C., Hubert, C. G., Gillespie, S. M., Flavahan, W. A., Hoffmann, T., Thummalapalli, R., Hemann, M. T., Paddison, P. J., Horbinski, C. M., … Rich, J. N. (2017). Transcription elongation factors represent in vivo cancer dependencies in glioblastoma. *Nature*, *547*(7663), 355–359. https://doi.org/10.1038/nature23000

Moffat, J., & Sabatini, D. M. (2006). Building mammalian signalling pathways with RNAi screens. In *Nature Reviews Molecular Cell Biology*. https://doi.org/10.1038/nrm1860

Mohammadi, M., Cao, Y., Glimelius, I., Bottai, M., Eloranta, S., & Smedby, K. E. (2015). The impact of comorbid disease history on all-cause and cancer-specific mortality in myeloid leukemia and myeloma - a Swedish population-based study. *BMC Cancer*, *15*, 850. https://doi.org/10.1186/s12885-015-1857-x

Mojica, F. J.M., Díez-Villaseñor, C., García-Martínez, J., & Almendros, C. (2009). Short motif sequences determine the targets of the prokaryotic CRISPR defence system. *Microbiology*. https://doi.org/10.1099/mic.0.023960-0

Mojica, F. J M, Díez-Villaseñor, C., García-Martínez, J., & Soria, E. (2005). Intervening sequences of regularly spaced prokaryotic repeats derive from foreign genetic elements. *Journal of Molecular Evolution*, *60*(2), 174–182. https://doi.org/10.1007/s00239-004-0046-3

Mojica, Francisco J. M., Diez-Villasenor, C., Soria, E., & Juez, G. (2000). Biological significance of a family of regularly spaced repeats in the genomes of Archaea, Bacteria and mitochondria. *Molecular Microbiology*, *36*(1), 244–246. https://doi.org/10.1046/j.1365-2958.2000.01838.x

Moreno-Smith, M., Lu, C., Shahzad, M. M. K., Pena, G. N. A., Allen, J. K., Stone, R. L., Mangala, L. S., Han, H. D., Kim, H. S., Farley, D., Berestein, G. L., Cole, S. W., Lutgendorf, S. K., & Sood, A. K. (2011). Dopamine blocks stress-mediated ovarian carcinoma growth. *Clinical Cancer Research : An Official Journal of the American Association for Cancer Research*, *17*(11), 3649–3659. https://doi.org/10.1158/1078-0432.CCR-10-2441

Ng, S., Gisonni-Lex, L., & Azizi, A. (2017). New approaches for characterization of the genetic stability of vaccine cell lines. In *Human Vaccines and Immunotherapeutics*. https://doi.org/10.1080/21645515.2017.1295191

Ng, S. W. K., Mitchell, A., Kennedy, J. A., Chen, W. C., McLeod, J., Ibrahimova, N., Arruda, A., Popescu, A., Gupta, V., Schimmer, A. D., Schuh, A. C., Yee, K. W., Bullinger, L., Herold, T., Görlich, D., Büchner, T., Hiddemann, W., Berdel, W. E., Wörmann, B., …

Wang, J. C. Y. (2016). A 17-gene stemness score for rapid determination of risk in acute leukaemia. *Nature*, *540*(7633), 433–437. https://doi.org/10.1038/nature20598

Omsland, M., Bruserud, Ø., Gjertsen, B. T., & Andresen, V. (2017). Tunneling nanotube (TNT) formation is downregulated by cytarabine and NF-κB inhibition in acute myeloid leukemia (AML). *Oncotarget*, *8*(5), 7946–7963. https://doi.org/10.18632/oncotarget.13853

Paddison, P. J., Silva, J. M., Conklin, D. S., Schlabach, M., Li, M., Aruleba, S., Balija, V., O'Shaughnessy, A., Gnoj, L., Scoble, K., Chang, K., Westbrook, T., Cleary, M., Sachidanandam, R., McComble, W. R., Elledge, S. J., & Hannon, G. J. (2004). A resource for large-scale RNA-interference-based screens in mammals. *Nature*. https://doi.org/10.1038/nature02370

Parnas, O., Jovanovic, M., Eisenhaure, T. M., Herbst, R. H., Dixit, A., Ye, C. J., Przybylski, D., Platt, R. J., Tirosh, I., Sanjana, N. E., Shalem, O., Satija, R., Raychowdhury, R., Mertins, P., Carr, S. A., Zhang, F., Hacohen, N., & Regev, A. (2015). A Genome-wide CRISPR Screen in Primary Immune Cells to Dissect Regulatory Networks. *Cell*. https://doi.org/10.1016/j.cell.2015.06.059

Pikman, Y., Puissant, A., Alexe, G., Furman, A., Chen, L. M., Frumm, S. M., Ross, L., Fenouille, N., Bassil, C. F., Lewis, C. A., Ramos, A., Gould, J., Stone, R. M., DeAngelo, D. J., Galinsky, I., Clish, C. B., Kung, A. L., Hemann, M. T., Vander Heiden, M. G., … Stegmaier, K. (2016). Targeting MTHFD2 in acute myeloid leukemia. *The Journal of Experimental Medicine*, *213*(7), 1285–1306. https://doi.org/10.1084/jem.20151574

Pornour, M., Ahangari, G., Hejazi, S. H., Ahmadkhaniha, H. R., & Akbari, M. E. (2015). Dopamine Receptor Gene (DRD1-DRD5) Expression Changes as Stress Factors Associated with Breast Cancer. *Asian Pacific Journal of Cancer Prevention*, *15*(23), 10339–10343. https://doi.org/10.7314/APJCP.2014.15.23.10339

Qin, J. Y., Zhang, L., Clift, K. L., Hulur, I., Xiang, A. P., Ren, B. Z., & Lahn, B. T. (2010). Systematic comparison of constitutive promoters and the doxycycline-inducible promoter. *PLoS ONE*. https://doi.org/10.1371/journal.pone.0010611

Rao, R. N., Allen, N. E., Hobbs, J. N., Alborn, W. E., Kirst, H. A., & Paschal, J. W. (1983). Genetic and enzymatic basis of hygromycin B resistance in Escherichia coli. *Antimicrobial Agents and Chemotherapy*. https://doi.org/10.1128/AAC.24.5.689

Risueño, R. M., Campbell, C. J. V., Dingwall, S., Levadoux-Martin, M., Leber, B., Xenocostas, A., & Bhatia, M. (2011). Identification of T-lymphocytic leukemia - Initiating stem cells residing in a small subset of patients with acute myeloid leukemic disease. *Blood*. https://doi.org/10.1182/blood-2011-01-329078

Robak, T., & Wierzbowska, A. (2009). Current and emerging therapies for acute myeloid leukemia. *Clinical Therapeutics*, *31*, 2349–2370. https://doi.org/10.1016/J.CLINTHERA.2009.11.017

Roddie, P. H., Paterson, T., & Turner, M. L. (2000). Gene transfer to primary acute myeloid leukaemia blasts and myeloid leukaemia cell lines. *Cytokines, Cellular & Molecular Therapy*, *6*(3), 127–134. http://www.ncbi.nlm.nih.gov/pubmed/11140881

Rodríguez-Rodríguez, D. R., Ramírez-Solís, R., Garza-Elizondo, M. A., Garza-Rodríguez, M. D. L., & Barrera-Saldaña, H. A. (2019). Genome editing: A perspective on the application of CRISPR/Cas9 to study human diseases (Review). In *International Journal of Molecular Medicine*. https://doi.org/10.3892/ijmm.2019.4112

Root, D. E., Hacohen, N., Hahn, W. C., Lander, E. S., & Sabatini, D. M. (2006). Genome-scale loss-of-function screening with a lentiviral RNAi library. *Nature Methods*.

https://doi.org/10.1038/nmeth924
Roth, D. B. (2014). V(D)J Recombination: Mechanism, Errors, and Fidelity. *Microbiology Spectrum*. https://doi.org/10.1128/microbiolspec.mdna3-0041-2014
Saland, E., Boutzen, H., Castellano, R., Pouyet, L., Griessinger, E., Larrue, C., de Toni, F., Scotland, S., David, M., Danet-Desnoyers, G., Vergez, F., Barreira, Y., Collette, Y., Récher, C., & Sarry, J.-E. (2015). A robust and rapid xenograft model to assess efficacy of chemotherapeutic agents for human acute myeloid leukemia. *Blood Cancer Journal*, *5*(3), e297. https://doi.org/10.1038/bcj.2015.19
Sampath, D., Rao, V. A., & Plunkett, W. (2003). Mechanisms of apoptosis induction by nucleoside analogs. In *Oncogene*. https://doi.org/10.1038/sj.onc.1207229
Sanchez, P. V., Perry, R. L., Sarry, J. E., Perl, A. E., Murphy, K., Swider, C. R., Bagg, A., Choi, J. K., Biegel, J. A., Danet-Desnoyers, G., & Carroll, M. (2009). A robust xenotransplantation model for acute myeloid leukemia. *Leukemia*. https://doi.org/10.1038/leu.2009.143
Saultz, J. N., & Garzon, R. (2016). Acute Myeloid Leukemia: A Concise Review. *Journal of Clinical Medicine*, *5*(3). https://doi.org/10.3390/jcm5030033
Scherer, A. (2009). Batch Effects and Noise in Microarray Experiments: Sources and Solutions. In *Batch Effects and Noise in Microarray Experiments: Sources and Solutions*. https://doi.org/10.1002/9780470685983
Shlush, L. I., Mitchell, A., Heisler, L., Abelson, S., Ng, S. W. K., Trotman-Grant, A., Medeiros, J. J. F., Rao-Bhatia, A., Jaciw-Zurakowsky, I., Marke, R., McLeod, J. L., Doedens, M., Bader, G., Voisin, V., Xu, C., McPherson, J. D., Hudson, T. J., Wang, J. C. Y., Minden, M. D., & Dick, J. E. (2017). Tracing the origins of relapse in acute myeloid leukaemia to stem cells. *Nature*, *547*(7661), 104–108. https://doi.org/10.1038/nature22993
Shlush, L. I., Zandi, S., Mitchell, A., Chen, W. C., Brandwein, J. M., Gupta, V., Kennedy, J. A., Schimmer, A. D., Schuh, A. C., Yee, K. W., McLeod, J. L., Doedens, M., Medeiros, J. J. F., Marke, R., Kim, H. J., Lee, K., McPherson, J. D., Hudson, T. J., Pan-Leukemia Gene Panel Consortium, T. H., … Dick, J. E. (2014). Identification of pre-leukaemic haematopoietic stem cells in acute leukaemia. *Nature*, *506*(7488), 328–333. https://doi.org/10.1038/nature13038
Shultz, L. D., Lyons, B. L., Burzenski, L. M., Gott, B., Chen, X., Chaleff, S., Kotb, M., Gillies, S. D., King, M., Mangada, J., Greiner, D. L., & Handgretinger, R. (2005). Human Lymphoid and Myeloid Cell Development in NOD/LtSz- scid IL2R γ null Mice Engrafted with Mobilized Human Hemopoietic Stem Cells . *The Journal of Immunology*. https://doi.org/10.4049/jimmunol.174.10.6477
Sundström, C., & Nilsson, K. (1976). Establishment and characterization of a human histiocytic lymphoma cell line (U-937). *International Journal of Cancer*, *17*(5), 565–577. https://doi.org/10.1002/ijc.2910170504
Theocharides, A. P. A., Rongvaux, A., Fritsch, K., Flavell, R. A., & Manz, M. G. (2016). Humanized hemato-lymphoid system mice. *Haematologica*. https://doi.org/10.3324/haematol.2014.115212
TILL, J. E., & McCULLOCH, E. A. (1961). A direct measurement of the radiation sensitivity of normal mouse bone marrow cells. *Radiation Research*, *14*, 213–222. http://www.ncbi.nlm.nih.gov/pubmed/13776896
van Buul, J. D., Voermans, C., van Gelderen, J., Anthony, E. C., van der Schoot, C. E., & Hordijk, P. L. (2003). Leukocyte-endothelium interaction promotes SDF-1-dependent

polarization of CXCR4. *The Journal of Biological Chemistry*, *278*(32), 30302–30310. https://doi.org/10.1074/jbc.M304764200

Verma, D., Kantarjian, H., Faderl, S., O'Brien, S., Pierce, S., Vu, K., Freireich, E., Keating, M., Cortes, J., & Ravandi, F. (2010). Late relapses in acute myeloid leukemia: Analysis of characteristics and outcome. *Leukemia and Lymphoma*. https://doi.org/10.3109/10428191003661852

Wan, L., Wen, H., Li, Y., Lyu, J., Xi, Y., Hoshii, T., Joseph, J. K., Wang, X., Loh, Y.-H. E., Erb, M. A., Souza, A. L., Bradner, J. E., Shen, L., Li, W., Li, H., Allis, C. D., Armstrong, S. A., & Shi, X. (2017). ENL links histone acetylation to oncogenic gene expression in acute myeloid leukaemia. *Nature*, *543*(7644), 265–269. https://doi.org/10.1038/nature21687

Wang, L. D., & Wagers, A. J. (2011). Dynamic niches in the origination and differentiation of haematopoietic stem cells. *Nature Reviews Molecular Cell Biology*, *12*(10), 643–655. https://doi.org/10.1038/nrm3184

Xu, J., Zhang, W., Yan, X.-J., Lin, X.-Q., Li, W., Mi, J.-Q., Li, J.-M., Zhu, J., Chen, Z., & Chen, S.-J. (2016). DNMT3A mutation leads to leukemic extramedullary infiltration mediated by TWIST1. *Journal of Hematology & Oncology*, *9*(1), 106. https://doi.org/10.1186/s13045-016-0337-3

Yamaguchi, I., Shibata, H., Misato, T., & Seto, H. (1975). Isolation and purification of blasticidin s deaminase from aspergillus terreus. *The Journal of Antibiotics*. https://doi.org/10.7164/antibiotics.28.7

Almeida, A. M., & Ramos, F. (2016). Acute myeloid leukemia in the older adults. *Leukemia Research Reports*, *6*, 1–7. https://doi.org/10.1016/j.lrr.2016.06.001

Almosailleakh, M., & Schwaller, J. (2019). Murine models of acute Myeloid Leukaemia. In *International Journal of Molecular Sciences*. https://doi.org/10.3390/ijms20020453

Anders, C., Niewoehner, O., Duerst, A., & Jinek, M. (2014). Structural basis of PAM-dependent target DNA recognition by the Cas9 endonuclease. *Nature*. https://doi.org/10.1038/nature13579

Andresen, V., Erikstein, B. S., Mukherjee, H., Sulen, A., Popa, M., Sørnes, S., Reikvam, H., Chan, K.-P., Hovland, R., McCormack, E., Bruserud, Ø., Myers, A. G., & Gjertsen, B. T. (2016). Anti-proliferative activity of the NPM1 interacting natural product avrainvillamide in acute myeloid leukemia. *Cell Death & Disease*, *7*(12), e2497. https://doi.org/10.1038/cddis.2016.392

Aslostovar, L., Boyd, A. L., Almakadi, M., Collins, T. J., Leong, D. P., Tirona, R. G., Kim, R. B., Julian, J. A., Xenocostas, A., Leber, B., Levine, M. N., Foley, R., & Bhatia, M. (2018). A phase 1 trial evaluating thioridazine in combination with cytarabine in patients with acute myeloid leukemia. *Blood Advances*, *2*(15), 1935–1945. https://doi.org/10.1182/bloodadvances.2018015677

Bachas, C., Hodzic, J., van der Mijn, J. C., Stoepker, C., Verheul, H. M. W., Wolthuis, R. M. F., Felley-Bosco, E., van Wieringen, W. N., van Beusechem, V. W., Brakenhoff, R. H., & de Menezes, R. X. (2018). Rscreenorm: Normalization of CRISPR and siRNA screen data for more reproducible hit selection. *BMC Bioinformatics*. https://doi.org/10.1186/s12859-018-2306-z

Balusu, R., Fiskus, W., Rao, R., Chong, D. G., Nalluri, S., Mudunuru, U., Ma, H., Chen, L., Venkannagari, S., Ha, K., Abhyankar, S., Williams, C., McGuirk, J., Khoury, H. J., Ustun,

C., & Bhalla, K. N. (2011). Targeting levels or oligomerization of nucleophosmin 1 induces differentiation and loss of survival of human AML cells with mutant NPM1. *Blood*, *118*(11), 3096–3106. https://doi.org/10.1182/blood-2010-09-309674

Berns, K., Hijmans, E. M., Mullenders, J., Brummelkamp, T. R., Velds, A., Heimerikx, M., Kerkhoven, R. M., Madlredjo, M., Nijkamp, W., Weigelt, B., Agami, R., Ge, W., Cavet, G., Linsley, P. S., Beijersbergen, R. L., & Bernards, R. (2004). A large-scale RNAi screen in human cells identifies new components of the p53 pathway. *Nature*. https://doi.org/10.1038/nature02371

Bierhuizen, M. F., Westerman, Y., Hartong, S. C., Visser, T. P., Wognum, A. W., & Wagemaker, G. (1999). Efficient detection and selection of immature rhesus monkey and human CD34+ hematopoietic cells expressing the enhanced green fluorescent protein (EGFP). *Leukemia*. https://doi.org/10.1038/sj.leu.2401374

Boettcher, M., & McManus, M. T. (2015). Choosing the Right Tool for the Job: RNAi, TALEN, or CRISPR. In *Molecular Cell*. https://doi.org/10.1016/j.molcel.2015.04.028

Bonnet, D., & Dick, J. E. (1997). Human acute myeloid leukemia is organized as a hierarchy that originates from a primitive hematopoietic cell. *Nature Medicine*. https://doi.org/10.1038/nm0797-730

Borthakur, G., Duvvuri, S., Ruvolo, V., Tripathi, D. N., Piya, S., Burks, J., Jacamo, R., Kojima, K., Ruvolo, P., Fueyo-Margareto, J., Konopleva, M., & Andreeff, M. (2015). MDM2 Inhibitor, Nutlin 3a, Induces p53 Dependent Autophagy in Acute Leukemia by AMP Kinase Activation. *PloS One*, *10*(10), e0139254. https://doi.org/10.1371/journal.pone.0139254

Bose, P., Vachhani, P., & Cortes, J. E. (2017). Treatment of Relapsed/Refractory Acute Myeloid Leukemia. *Current Treatment Options in Oncology*, *18*(3), 17. https://doi.org/10.1007/s11864-017-0456-2

Boutros, M., Kiger, A. A., Armknecht, S., Kerr, K., Hild, M., Koch, B., Haas, S. A., Paro, R., & Perrimon, N. (2004). Genome-Wide RNAi Analysis of Growth and Viability in Drosophila Cells. *Science*. https://doi.org/10.1126/science.1091266

Box, J. K., Paquet, N., Adams, M. N., Boucher, D., Bolderson, E., O'Byrne, K. J., & Richard, D. J. (2016). Nucleophosmin: from structure and function to disease development. *BMC Molecular Biology*, *17*(1), 19. https://doi.org/10.1186/s12867-016-0073-9

Boyd, A. L., Aslostovar, L., Reid, J., Ye, W., Tanasijevic, B., Porras, D. P., Shapovalova, Z., Almakadi, M., Foley, R., Leber, B., Xenocostas, A., & Bhatia, M. (2018). Identification of Chemotherapy-Induced Leukemic-Regenerating Cells Reveals a Transient Vulnerability of Human AML Recurrence. *Cancer Cell*, *34*(3), 483-498.e5. https://doi.org/10.1016/J.CCELL.2018.08.007

Bryder, D., Rossi, D. J., & Weissman, I. L. (2006). Hematopoietic stem cells: The paradigmatic tissue-specific stem cell. *American Journal of Pathology*. https://doi.org/10.2353/ajpath.2006.060312

Burger, O., Ashtamker, G. F., Bercovich, N., Rusanovsky, M., Pinzur, L., Jacov, O. M., Carmi, N. D., Meiron, M., Lior, L., Meretzki, S., Prather, W. R., Kadouri, A., Treves, A. J., Rowe, J. M., Horwitz, E. M., & Nagler, A. (2007). Human Placental Derived Mesenchymal Stromal Cells (MSC) Grown in 3D-Culture (PLX-I), Promotes Engraftment of Human Umbilical Cord Blood (hUCB) Derived CD34+ Cells in NOD/SCID Mice. *Blood*. https://doi.org/10.1182/blood.v110.11.1416.1416

Caldarelli, A., Müller, J. P., Paskowski-Rogacz, M., Herrmann, K., Bauer, R., Koch, S., Heninger, A. K., Krastev, D., Ding, L., Kasper, S., Fischer, T., Brodhun, M., Böhmer, F.-

D., & Buchholz, F. (2013). A genome-wide RNAi screen identifies proteins modulating aberrant FLT3-ITD signaling. *Leukemia*, *27*(12), 2301–2310. https://doi.org/10.1038/leu.2013.83

Cao, X., Shores, E. W., Hu-Li, J., Anver, M. R., Kelsail, B. L., Russell, S. M., Drago, J., Noguchi, M., Grinberg, A., Bloom, E. T., Paul, W. E., Katz, S. I., Love, P. E., & Leonard, W. J. (1995). Defective lymphoid development in mice lacking expression of the common cytokine receptor γ chain. *Immunity*. https://doi.org/10.1016/1074-7613(95)90047-0

Caocci, G., Greco, M., & La Nasa, G. (2017). Bone Marrow Homing and Engraftment Defects of Human Hematopoietic Stem and Progenitor Cells. *Mediterranean Journal of Hematology and Infectious Diseases*, *9*(1), e2017032. https://doi.org/10.4084/MJHID.2017.032

CHANG, H.-Y., RODRIGUEZ, V., NARBONI, G., BODEY, G. P., LUNA, M. A., & FREIREICH, E. J. (1976). CAUSES OF DEATH IN ADULTS WITH ACUTE LEUKEMIA. *Medicine*, *55*(3), 259–268. https://doi.org/10.1097/00005792-197605000-00005

Chen, S., Sanjana, N. E., Zheng, K., Shalem, O., Lee, K., Shi, X., Scott, D. A., Song, J., Pan, J. Q., Weissleder, R., Lee, H., Zhang, F., & Sharp, P. A. (2015). Genome-wide CRISPR screen in a mouse model of tumor growth and metastasis. *Cell*. https://doi.org/10.1016/j.cell.2015.02.038

Chen, Y.-L., Chueh, F.-S., Yang, J.-S., Hsueh, S.-C., Lu, C.-C., Chiang, J.-H., Lee, C.-S., Lu, H.-F., & Chung, J.-G. (2015). Antitumor effects with apoptotic death in human promyelocytic leukemia HL-60 cells and suppression of leukemia xenograft tumor growth by irinotecan HCl. *Environmental Toxicology*, *30*(7), 803–815. https://doi.org/10.1002/tox.21959

Cho, B.-S., Zeng, Z., Mu, H., Wang, Z., Konoplev, S., McQueen, T., Protopopova, M., Cortes, J., Marszalek, J. R., Peng, S.-B., Ma, W., Davis, R. E., Thornton, D. E., Andreeff, M., & Konopleva, M. (2015). Antileukemia activity of the novel peptidic CXCR4 antagonist LY2510924 as monotherapy and in combination with chemotherapy. *Blood*, *126*(2), 222–232. https://doi.org/10.1182/blood-2015-02-628677

Cline, S. D., & Osheroff, N. (1999). Cytosine arabinoside lesions are position-specific topoisomerase II poisons and stimulate DNA cleavage mediated by the human type II enzymes. *The Journal of Biological Chemistry*, *274*(42), 29740–29743. https://doi.org/10.1074/jbc.274.42.29740

Cohen, S. S. (1977). The mechanisms of lethal action of arabinosyl cytosine (araC) and arabinosyl adenine (araA). *Cancer*, *40*(1 Suppl), 509–518. http://www.ncbi.nlm.nih.gov/pubmed/328134

Colvin, G. A., Lambert, J. F., Abedi, M., Hsieh, C. C., Carlson, J. E., Stewart, F. M., & Quesenberry, P. J. (2004). Murine marrow cellularity and the concept of stem cell competition: Geographic and quantitative determinants in stem cell biology. *Leukemia*. https://doi.org/10.1038/sj.leu.2403268

Corces, M. R., Buenrostro, J. D., Wu, B., Greenside, P. G., Chan, S. M., Koenig, J. L., Snyder, M. P., Pritchard, J. K., Kundaje, A., Greenleaf, W. J., Majeti, R., & Chang, H. Y. (2016). Lineage-specific and single-cell chromatin accessibility charts human hematopoiesis and leukemia evolution. *Nature Genetics*, *48*(10), 1193–1203. https://doi.org/10.1038/ng.3646

Damaraju, V. L., Damaraju, S., Young, J. D., Baldwin, S. A., Mackey, J., Sawyer, M. B., & Cass, C. E. (2003). Nucleoside anticancer drugs: The role of nucleoside transporters in resistance to cancer chemotherapy. In *Oncogene*. https://doi.org/10.1038/sj.onc.1206952

De Greef, G. E., Van Putten, W. L. J., Boogaerts, M., Huijgens, P. C., Verdonck, L. F., Vellenga,

E., Theobald, M., Jacky, E., & Löwenberg, B. (2005). Criteria for defining a complete remission in acute myeloid leukaemia revisited. An analysis of patients treated in HOVON-SAKK co-operative group studies. *British Journal of Haematology*. https://doi.org/10.1111/j.1365-2141.2004.05285.x

De Kouchkovsky, I., & Abdul-Hay, M. (2016). 'Acute myeloid leukemia: a comprehensive review and 2016 update.' *Blood Cancer Journal*, *6*(7), e441–e441. https://doi.org/10.1038/bcj.2016.50

Deslauriers, J., Lefrançois, M., Larouche, A., Sarret, P., & Grignon, S. (2011). Antipsychotic-induced DRD2 upregulation and its prevention by α-lipoic acid in SH-SY5Y neuroblastoma cells. *Synapse (New York, N.Y.)*, *65*(4), 321–331. https://doi.org/10.1002/syn.20851

Döhner, H., Estey, E., Grimwade, D., Amadori, S., Appelbaum, F. R., Büchner, T., Dombret, H., Ebert, B. L., Fenaux, P., Larson, R. A., Levine, R. L., Lo-Coco, F., Naoe, T., Niederwieser, D., Ossenkoppele, G. J., Sanz, M., Sierra, J., Tallman, M. S., Tien, H. F., … Bloomfield, C. D. (2017). Diagnosis and management of AML in adults: 2017 ELN recommendations from an international expert panel. In *Blood* (Vol. 129, Issue 4, pp. 424–447). American Society of Hematology. https://doi.org/10.1182/blood-2016-08-733196

Döhner, H., Weisdorf, D. J., & Bloomfield, C. D. (2015). Acute Myeloid Leukemia. *New England Journal of Medicine*, *373*(12), 1136–1152. https://doi.org/10.1056/NEJMra1406184

Duran-Struuck, R., & Dysko, R. C. (2009). Principles of bone marrow transplantation (BMT): Providing optimal veterinary and husbandry care to irradiated mice in BMT studies. In *Journal of the American Association for Laboratory Animal Science*.

Farge, T., Saland, E., de Toni, F., Aroua, N., Hosseini, M., Perry, R., Bosc, C., Sugita, M., Stuani, L., Fraisse, M., Scotland, S., Larrue, C., Boutzen, H., Féliu, V., Nicolau-Travers, M.-L., Cassant-Sourdy, S., Broin, N., David, M., Serhan, N., … Sarry, J.-E. (2017a). Chemotherapy-Resistant Human Acute Myeloid Leukemia Cells Are Not Enriched for Leukemic Stem Cells but Require Oxidative Metabolism. *Cancer Discovery*, *7*(7), 716–735. https://doi.org/10.1158/2159-8290.CD-16-0441

Farge, T., Saland, E., de Toni, F., Aroua, N., Hosseini, M., Perry, R., Bosc, C., Sugita, M., Stuani, L., Fraisse, M., Scotland, S., Larrue, C., Boutzen, H., Féliu, V., Nicolau-Travers, M.-L., Cassant-Sourdy, S., Broin, N., David, M., Serhan, N., … Sarry, J.-E. (2017b). Chemotherapy-Resistant Human Acute Myeloid Leukemia Cells Are Not Enriched for Leukemic Stem Cells but Require Oxidative Metabolism. *Cancer Discovery*, *7*(7), 716–735. https://doi.org/10.1158/2159-8290.CD-16-0441

Floc'h, N., Ashton, S., Taylor, P., Trueman, D., Harris, E., Odedra, R., Maratea, K., Derbyshire, N., Caddy, J., Jacobs, V. N., Hattersley, M., Wen, S., Curtis, N. J., Pilling, J. E., Pease, E. J., & Barry, S. T. (2017). *Optimizing Therapeutic Effect of Aurora B Inhibition in Acute Myeloid Leukemia with AZD2811 Nanoparticles*. https://doi.org/10.1158/1535-7163.MCT-16-0580

Garneau, J. E., Dupuis, M. È., Villion, M., Romero, D. A., Barrangou, R., Boyaval, P., Fremaux, C., Horvath, P., Magadán, A. H., & Moineau, S. (2010). The CRISPR/cas bacterial immune system cleaves bacteriophage and plasmid DNA. *Nature*. https://doi.org/10.1038/nature09523

Green, A. S., Maciel, T. T., Hospital, M.-A., Yin, C., Mazed, F., Townsend, E. C., Pilorge, S., Lambert, M., Paubelle, E., Jacquel, A., Zylbersztejn, F., Decroocq, J., Poulain, L., Sujobert, P., Jacque, N., Adam, K., So, J. C. C., Kosmider, O., Auberger, P., … Tamburini, J. (2015).

Pim kinases modulate resistance to FLT3 tyrosine kinase inhibitors in FLT3-ITD acute myeloid leukemia. *Science Advances*, *1*(8), e1500221. https://doi.org/10.1126/sciadv.1500221

He, L., Shi, L., Du, Z., Huang, H., Gong, R., Ma, L., Chen, L., Gao, S., Lyu, J., & Gu, H. (2018). Mebendazole exhibits potent anti-leukemia activity on acute myeloid leukemia. *Experimental Cell Research*, *369*(1), 61–68. https://doi.org/10.1016/J.YEXCR.2018.05.006

Heydt, Q., Larrue, C., Saland, E., Bertoli, S., Sarry, J.-E., Besson, A., Manenti, S., Joffre, C., & Mansat-De Mas, V. (2018). Oncogenic FLT3-ITD supports autophagy via ATF4 in acute myeloid leukemia. *Oncogene*, *37*(6), 787–797. https://doi.org/10.1038/onc.2017.376

Hicks, S. C., & Irizarry, R. A. (2014). When to use Quantile Normalization? *BioRxiv*. https://doi.org/10.1101/012203

Ishino, Y., Shinagawa, H., Makino, K., Amemura, M., & Nakata, A. (1987). Nucleotide sequence of the iap gene, responsible for alkaline phosphatase isozyme conversion in Escherichia coli, and identification of the gene product. *Journal of Bacteriology*, *169*(12), 5429–5433. https://doi.org/10.1128/jb.169.12.5429-5433.1987

Ito, M., Hiramatsu, H., Kobayashi, K., Suzue, K., Kawahata, M., Hioki, K., Ueyama, Y., Koyanagi, Y., Sugamura, K., Tsuji, K., Heike, T., & Nakahata, T. (2002). NOD/SCID/γcnull mouse: An excellent recipient mouse model for engraftment of human cells. *Blood*. https://doi.org/10.1182/blood-2001-12-0207

Jagannathan-Bogdan, M., & Zon, L. I. (2013). Hematopoiesis. *Development (Cambridge, England)*, *140*(12), 2463–2467. https://doi.org/10.1242/dev.083147

Jansen, R., Van Embden, J. D. A., Gaastra, W., & Schouls, L. M. (2002). Identification of genes that are associated with DNA repeats in prokaryotes. *Molecular Microbiology*, *43*(6), 1565–1575. https://doi.org/10.1046/j.1365-2958.2002.02839.x

Jian, P., Li, Z. W., Fang, T. Y., Jian, W., Zhuan, Z., Mei, L. X., Yan, W. S., & Jian, N. (2011). Retinoic acid induces HL-60 cell differentiation via the upregulation of miR-663. *Journal of Hematology & Oncology*, *4*, 20. https://doi.org/10.1186/1756-8722-4-20

Jinek, M., Chylinski, K., Fonfara, I., Hauer, M., Doudna, J. A., & Charpentier, E. (2012). A programmable dual-RNA-guided DNA endonuclease in adaptive bacterial immunity. *Science*. https://doi.org/10.1126/science.1225829

Joung, J., Konermann, S., Gootenberg, J. S., Abudayyeh, O. O., Platt, R. J., Brigham, M. D., Sanjana, N. E., & Zhang, F. (2017). Genome-scale CRISPR-Cas9 knockout and transcriptional activation screening. *Nature Protocols*, *12*(4), 828–863. https://doi.org/10.1038/nprot.2017.016

Kanakis, G., Grimelius, L., Spathis, A., Tringidou, R., Rassidakis, G. Z., Öberg, K., Kaltsas, G., & Tsolakis, A. V. (2015). Expression of Somatostatin Receptors 1-5 and Dopamine Receptor 2 in Lung Carcinoids: Implications for a Therapeutic Role. *Neuroendocrinology*, *101*(3), 211–222. https://doi.org/10.1159/000381061

Khwaja, A., Bjorkholm, M., Gale, R. E., Levine, R. L., Jordan, C. T., Ehninger, G., Bloomfield, C. D., Estey, E., Burnett, A., Cornelissen, J. J., Scheinberg, D. A., Bouscary, D., & Linch, D. C. (2016). Acute myeloid leukaemia. *Nature Reviews Disease Primers*, *2*, 16010. https://doi.org/10.1038/nrdp.2016.10

Konermann, S., Brigham, M. D., Trevino, A. E., Joung, J., Abudayyeh, O. O., Barcena, C., Hsu, P. D., Habib, N., Gootenberg, J. S., Nishimasu, H., Nureki, O., & Zhang, F. (2015). Genome-scale transcriptional activation by an engineered CRISPR-Cas9 complex. *Nature*, *517*(7536), 583–588. https://doi.org/10.1038/nature14136

König, R., Chiang, C. Y., Tu, B. P., Yan, S. F., DeJesus, P. D., Romero, A., Bergauer, T., Orth, A., Krueger, U., Zhou, Y., & Chanda, S. K. (2007). A probability-based approach for the analysis of large-scale RNAi screens. *Nature Methods*. https://doi.org/10.1038/nmeth1089

Kumar, C. C. (2011). Genetic abnormalities and challenges in the treatment of acute myeloid leukemia. *Genes & Cancer*, *2*(2), 95–107. https://doi.org/10.1177/1947601911408076

L.D., S., M.A., B., J., V. G.-M., & D.L., G. (2012). Humanized mice for immune system investigation: Progress, promise and challenges. In *Nature Reviews Immunology*.

Li, B., Clohisey, S. M., Chia, B. S., Wang, B., Cui, A., Eisenhaure, T., Schweitzer, L. D., Hoover, P., Parkinson, N. J., Nachshon, A., Smith, N., Regan, T., Farr, D., Gutmann, M. U., Bukhari, S. I., Law, A., Sangesland, M., Gat-Viks, I., Digard, P., … Hacohen, N. (2020). Genome-wide CRISPR screen identifies host dependency factors for influenza A virus infection. *Nature Communications*. https://doi.org/10.1038/s41467-019-13965-x

Li, J., Zhu, S., Kozono, D., Ng, K., Futalan, D., Shen, Y., Akers, J. C., Steed, T., Kushwaha, D., Schlabach, M., Carter, B. S., Kwon, C.-H., Furnari, F., Cavenee, W., Elledge, S., & Chen, C. C. (2014). Genome-wide shRNA screen revealed integrated mitogenic signaling between dopamine receptor D2 (DRD2) and epidermal growth factor receptor (EGFR) in glioblastoma. *Oncotarget*, *5*(4), 882–893. https://doi.org/10.18632/oncotarget.1801

Li, L., Miyamoto, M., Ebihara, Y., Mega, S., Takahashi, R., Hase, R., Kaneko, H., Kadoya, M., Itoh, T., Shichinohe, T., Hirano, S., & Kondo, S. (2006). DRD2/DARPP-32 expression correlates with lymph node metastasis and tumor progression in patients with esophageal squamous cell carcinoma. *World Journal of Surgery*, *30*(9), 1672–1679; discussion 1680-1. https://doi.org/10.1007/s00268-006-0035-3

Li, S., Mason, C. E., & Melnick, A. (2016). Genetic and epigenetic heterogeneity in acute myeloid leukemia. *Current Opinion in Genetics & Development*, *36*, 100–106. https://doi.org/10.1016/j.gde.2016.03.011

Mambet, C., Chivu-Economescu, M., Matei, L., Necula, L. G., Dragu, D. L., Bleotu, C., & Diaconu, C. C. (2018). Murine models based on acute myeloid leukemia-initiating stem cells xenografting. *World Journal of Stem Cells*, *10*(6), 57–65. https://doi.org/10.4252/wjsc.v10.i6.57

Mao, M., Yu, T., Hu, J., & Hu, L. (2015). Dopamine D2 receptor blocker thioridazine induces cell death in human uterine cervical carcinoma cell line SiHa. *Journal of Obstetrics and Gynaecology Research*, *41*(8), 1240–1245. https://doi.org/10.1111/jog.12691

Miller, T. E., Liau, B. B., Wallace, L. C., Morton, A. R., Xie, Q., Dixit, D., Factor, D. C., Kim, L. J. Y., Morrow, J. J., Wu, Q., Mack, S. C., Hubert, C. G., Gillespie, S. M., Flavahan, W. A., Hoffmann, T., Thummalapalli, R., Hemann, M. T., Paddison, P. J., Horbinski, C. M., … Rich, J. N. (2017). Transcription elongation factors represent in vivo cancer dependencies in glioblastoma. *Nature*, *547*(7663), 355–359. https://doi.org/10.1038/nature23000

Moffat, J., & Sabatini, D. M. (2006). Building mammalian signalling pathways with RNAi screens. In *Nature Reviews Molecular Cell Biology*. https://doi.org/10.1038/nrm1860

Mohammadi, M., Cao, Y., Glimelius, I., Bottai, M., Eloranta, S., & Smedby, K. E. (2015). The impact of comorbid disease history on all-cause and cancer-specific mortality in myeloid leukemia and myeloma - a Swedish population-based study. *BMC Cancer*, *15*, 850. https://doi.org/10.1186/s12885-015-1857-x

Mojica, F. J.M., Díez-Villaseñor, C., García-Martínez, J., & Almendros, C. (2009). Short motif sequences determine the targets of the prokaryotic CRISPR defence system. *Microbiology*. https://doi.org/10.1099/mic.0.023960-0

Mojica, F. J M, Díez-Villaseñor, C., García-Martínez, J., & Soria, E. (2005). Intervening sequences of regularly spaced prokaryotic repeats derive from foreign genetic elements. *Journal of Molecular Evolution*, *60*(2), 174–182. https://doi.org/10.1007/s00239-004-0046-3

Mojica, Francisco J. M., Diez-Villasenor, C., Soria, E., & Juez, G. (2000). Biological significance of a family of regularly spaced repeats in the genomes of Archaea, Bacteria and mitochondria. *Molecular Microbiology*, *36*(1), 244–246. https://doi.org/10.1046/j.1365-2958.2000.01838.x

Moreno-Smith, M., Lu, C., Shahzad, M. M. K., Pena, G. N. A., Allen, J. K., Stone, R. L., Mangala, L. S., Han, H. D., Kim, H. S., Farley, D., Berestein, G. L., Cole, S. W., Lutgendorf, S. K., & Sood, A. K. (2011). Dopamine blocks stress-mediated ovarian carcinoma growth. *Clinical Cancer Research : An Official Journal of the American Association for Cancer Research*, *17*(11), 3649–3659. https://doi.org/10.1158/1078-0432.CCR-10-2441

Ng, S., Gisonni-Lex, L., & Azizi, A. (2017). New approaches for characterization of the genetic stability of vaccine cell lines. In *Human Vaccines and Immunotherapeutics*. https://doi.org/10.1080/21645515.2017.1295191

Ng, S. W. K., Mitchell, A., Kennedy, J. A., Chen, W. C., McLeod, J., Ibrahimova, N., Arruda, A., Popescu, A., Gupta, V., Schimmer, A. D., Schuh, A. C., Yee, K. W., Bullinger, L., Herold, T., Görlich, D., Büchner, T., Hiddemann, W., Berdel, W. E., Wörmann, B., … Wang, J. C. Y. (2016). A 17-gene stemness score for rapid determination of risk in acute leukaemia. *Nature*, *540*(7633), 433–437. https://doi.org/10.1038/nature20598

Omsland, M., Bruserud, Ø., Gjertsen, B. T., & Andresen, V. (2017). Tunneling nanotube (TNT) formation is downregulated by cytarabine and NF-κB inhibition in acute myeloid leukemia (AML). *Oncotarget*, *8*(5), 7946–7963. https://doi.org/10.18632/oncotarget.13853

Paddison, P. J., Silva, J. M., Conklin, D. S., Schlabach, M., Li, M., Aruleba, S., Balija, V., O'Shaughnessy, A., Gnoj, L., Scoble, K., Chang, K., Westbrook, T., Cleary, M., Sachidanandam, R., McComble, W. R., Elledge, S. J., & Hannon, G. J. (2004). A resource for large-scale RNA-interference-based screens in mammals. *Nature*. https://doi.org/10.1038/nature02370

Parnas, O., Jovanovic, M., Eisenhaure, T. M., Herbst, R. H., Dixit, A., Ye, C. J., Przybylski, D., Platt, R. J., Tirosh, I., Sanjana, N. E., Shalem, O., Satija, R., Raychowdhury, R., Mertins, P., Carr, S. A., Zhang, F., Hacohen, N., & Regev, A. (2015). A Genome-wide CRISPR Screen in Primary Immune Cells to Dissect Regulatory Networks. *Cell*. https://doi.org/10.1016/j.cell.2015.06.059

Pikman, Y., Puissant, A., Alexe, G., Furman, A., Chen, L. M., Frumm, S. M., Ross, L., Fenouille, N., Bassil, C. F., Lewis, C. A., Ramos, A., Gould, J., Stone, R. M., DeAngelo, D. J., Galinsky, I., Clish, C. B., Kung, A. L., Hemann, M. T., Vander Heiden, M. G., … Stegmaier, K. (2016). Targeting MTHFD2 in acute myeloid leukemia. *The Journal of Experimental Medicine*, *213*(7), 1285–1306. https://doi.org/10.1084/jem.20151574

Pornour, M., Ahangari, G., Hejazi, S. H., Ahmadkhaniha, H. R., & Akbari, M. E. (2015). Dopamine Receptor Gene (DRD1-DRD5) Expression Changes as Stress Factors Associated with Breast Cancer. *Asian Pacific Journal of Cancer Prevention*, *15*(23), 10339–10343. https://doi.org/10.7314/APJCP.2014.15.23.10339

Qin, J. Y., Zhang, L., Clift, K. L., Hulur, I., Xiang, A. P., Ren, B. Z., & Lahn, B. T. (2010). Systematic comparison of constitutive promoters and the doxycycline-inducible promoter.

PLoS ONE. https://doi.org/10.1371/journal.pone.0010611

Rao, R. N., Allen, N. E., Hobbs, J. N., Alborn, W. E., Kirst, H. A., & Paschal, J. W. (1983). Genetic and enzymatic basis of hygromycin B resistance in Escherichia coli. *Antimicrobial Agents and Chemotherapy*. https://doi.org/10.1128/AAC.24.5.689

Risueño, R. M., Campbell, C. J. V., Dingwall, S., Levadoux-Martin, M., Leber, B., Xenocostas, A., & Bhatia, M. (2011). Identification of T-lymphocytic leukemia - Initiating stem cells residing in a small subset of patients with acute myeloid leukemic disease. *Blood*. https://doi.org/10.1182/blood-2011-01-329078

Robak, T., & Wierzbowska, A. (2009). Current and emerging therapies for acute myeloid leukemia. *Clinical Therapeutics*, *31*, 2349–2370. https://doi.org/10.1016/J.CLINTHERA.2009.11.017

Roddie, P. H., Paterson, T., & Turner, M. L. (2000). Gene transfer to primary acute myeloid leukaemia blasts and myeloid leukaemia cell lines. *Cytokines, Cellular & Molecular Therapy*, *6*(3), 127–134. http://www.ncbi.nlm.nih.gov/pubmed/11140881

Rodríguez-Rodríguez, D. R., Ramírez-Solís, R., Garza-Elizondo, M. A., Garza-Rodríguez, M. D. L., & Barrera-Saldaña, H. A. (2019). Genome editing: A perspective on the application of CRISPR/Cas9 to study human diseases (Review). In *International Journal of Molecular Medicine*. https://doi.org/10.3892/ijmm.2019.4112

Root, D. E., Hacohen, N., Hahn, W. C., Lander, E. S., & Sabatini, D. M. (2006). Genome-scale loss-of-function screening with a lentiviral RNAi library. *Nature Methods*. https://doi.org/10.1038/nmeth924

Roth, D. B. (2014). V(D)J Recombination: Mechanism, Errors, and Fidelity. *Microbiology Spectrum*. https://doi.org/10.1128/microbiolspec.mdna3-0041-2014

Saland, E., Boutzen, H., Castellano, R., Pouyet, L., Griessinger, E., Larrue, C., de Toni, F., Scotland, S., David, M., Danet-Desnoyers, G., Vergez, F., Barreira, Y., Collette, Y., Récher, C., & Sarry, J.-E. (2015). A robust and rapid xenograft model to assess efficacy of chemotherapeutic agents for human acute myeloid leukemia. *Blood Cancer Journal*, *5*(3), e297. https://doi.org/10.1038/bcj.2015.19

Sampath, D., Rao, V. A., & Plunkett, W. (2003). Mechanisms of apoptosis induction by nucleoside analogs. In *Oncogene*. https://doi.org/10.1038/sj.onc.1207229

Sanchez, P. V., Perry, R. L., Sarry, J. E., Perl, A. E., Murphy, K., Swider, C. R., Bagg, A., Choi, J. K., Biegel, J. A., Danet-Desnoyers, G., & Carroll, M. (2009). A robust xenotransplantation model for acute myeloid leukemia. *Leukemia*. https://doi.org/10.1038/leu.2009.143

Saultz, J. N., & Garzon, R. (2016). Acute Myeloid Leukemia: A Concise Review. *Journal of Clinical Medicine*, *5*(3). https://doi.org/10.3390/jcm5030033

Scherer, A. (2009). Batch Effects and Noise in Microarray Experiments: Sources and Solutions. In *Batch Effects and Noise in Microarray Experiments: Sources and Solutions*. https://doi.org/10.1002/9780470685983

Shlush, L. I., Mitchell, A., Heisler, L., Abelson, S., Ng, S. W. K., Trotman-Grant, A., Medeiros, J. J. F., Rao-Bhatia, A., Jaciw-Zurakowsky, I., Marke, R., McLeod, J. L., Doedens, M., Bader, G., Voisin, V., Xu, C., McPherson, J. D., Hudson, T. J., Wang, J. C. Y., Minden, M. D., & Dick, J. E. (2017). Tracing the origins of relapse in acute myeloid leukaemia to stem cells. *Nature*, *547*(7661), 104–108. https://doi.org/10.1038/nature22993

Shlush, L. I., Zandi, S., Mitchell, A., Chen, W. C., Brandwein, J. M., Gupta, V., Kennedy, J. A., Schimmer, A. D., Schuh, A. C., Yee, K. W., McLeod, J. L., Doedens, M., Medeiros, J. J. F.,

Marke, R., Kim, H. J., Lee, K., McPherson, J. D., Hudson, T. J., Pan-Leukemia Gene Panel Consortium, T. H., … Dick, J. E. (2014). Identification of pre-leukaemic haematopoietic stem cells in acute leukaemia. *Nature*, *506*(7488), 328–333. https://doi.org/10.1038/nature13038

Shultz, L. D., Lyons, B. L., Burzenski, L. M., Gott, B., Chen, X., Chaleff, S., Kotb, M., Gillies, S. D., King, M., Mangada, J., Greiner, D. L., & Handgretinger, R. (2005). Human Lymphoid and Myeloid Cell Development in NOD/LtSz- scid IL2R γ null Mice Engrafted with Mobilized Human Hemopoietic Stem Cells . *The Journal of Immunology*. https://doi.org/10.4049/jimmunol.174.10.6477

Sundström, C., & Nilsson, K. (1976). Establishment and characterization of a human histiocytic lymphoma cell line (U-937). *International Journal of Cancer*, *17*(5), 565–577. https://doi.org/10.1002/ijc.2910170504

Theocharides, A. P. A., Rongvaux, A., Fritsch, K., Flavell, R. A., & Manz, M. G. (2016). Humanized hemato-lymphoid system mice. *Haematologica*. https://doi.org/10.3324/haematol.2014.115212

TILL, J. E., & McCULLOCH, E. A. (1961). A direct measurement of the radiation sensitivity of normal mouse bone marrow cells. *Radiation Research*, *14*, 213–222. http://www.ncbi.nlm.nih.gov/pubmed/13776896

van Buul, J. D., Voermans, C., van Gelderen, J., Anthony, E. C., van der Schoot, C. E., & Hordijk, P. L. (2003). Leukocyte-endothelium interaction promotes SDF-1-dependent polarization of CXCR4. *The Journal of Biological Chemistry*, *278*(32), 30302–30310. https://doi.org/10.1074/jbc.M304764200

Verma, D., Kantarjian, H., Faderl, S., O'Brien, S., Pierce, S., Vu, K., Freireich, E., Keating, M., Cortes, J., & Ravandi, F. (2010). Late relapses in acute myeloid leukemia: Analysis of characteristics and outcome. *Leukemia and Lymphoma*. https://doi.org/10.3109/10428191003661852

Wan, L., Wen, H., Li, Y., Lyu, J., Xi, Y., Hoshii, T., Joseph, J. K., Wang, X., Loh, Y.-H. E., Erb, M. A., Souza, A. L., Bradner, J. E., Shen, L., Li, W., Li, H., Allis, C. D., Armstrong, S. A., & Shi, X. (2017). ENL links histone acetylation to oncogenic gene expression in acute myeloid leukaemia. *Nature*, *543*(7644), 265–269. https://doi.org/10.1038/nature21687

Wang, L. D., & Wagers, A. J. (2011). Dynamic niches in the origination and differentiation of haematopoietic stem cells. *Nature Reviews Molecular Cell Biology*, *12*(10), 643–655. https://doi.org/10.1038/nrm3184

Xu, J., Zhang, W., Yan, X.-J., Lin, X.-Q., Li, W., Mi, J.-Q., Li, J.-M., Zhu, J., Chen, Z., & Chen, S.-J. (2016). DNMT3A mutation leads to leukemic extramedullary infiltration mediated by TWIST1. *Journal of Hematology & Oncology*, *9*(1), 106. https://doi.org/10.1186/s13045-016-0337-3

Yamaguchi, I., Shibata, H., Misato, T., & Seto, H. (1975). Isolation and purification of blasticidin s deaminase from aspergillus terreus. *The Journal of Antibiotics*. https://doi.org/10.7164/antibiotics.28.7